Enhancement of radiation effects by high-Z nanoparticles

R. C. Carrillo-Torres, R. Meléndrez, V. Chernov,
M. Pedroza-Montero, R. García-Gutiérrez,
M. Barboza-Flores

July, 2012

Outline

- Motivation
- Radiotherapy
- Interaction of radiation with matter
- Dose enhancement by high-Z materials
- Gold nanoparticles
- Monte Carlo simulations
- *In vitro* studies
- *In vivo* studies
- Perspectives
- Conclusions
- Q&A

Motivation

- High-Z nanoparticles as radiosensitizing agents to enhance the effectiveness of radiation therapy protocols.

- The basis of radiosensitization relies mainly on increasing photoelectric absorption cross-section relative to tissue.

- In spite of the strong development of this field of nanotechnology some of the results obtained in cells lines and animals are controversial making difficult to fully understand the radiation dose enhancing effects.

- We review the current developments in nanoparticles suitable for therapeutic applications. It will be shown that the potential efficacy of nanoparticles radiosensitization is highly sensitive to a number of physics and pharmacological parameters including irradiation energy and nanoparticle size, concentration, and intracellular localization.

Radiotherapy

- Radiotherapy (RT) has become one of the primary tools to treat and prevent the spread of abnormal cancerous cells.

- Slightly more than 50% of all patients who developed cancer will require RT at some stage of their illness.

- RT utilizes ionizing radiations and has been used for several decades to treat a wide variety of cancer types.

Radiotherapy

- Kilovoltage x-ray sources
  - Low penetration
  - Delivered high dose
  - Low skin sparing effect
- LINACs
  - Higher energy x-ray and electron beams in megavoltage range
  - Nowadays, most common sources of ionizing radiation
  - Improved in dose distribution and effectiveness of RT

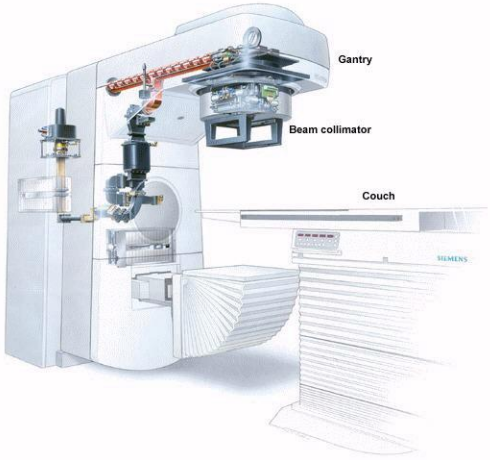

Radiotherapy

- Particle radiotherapy
  - Less common due to high installation cost
  - Better dose concentration
  - Has a proven role in the management of orbital tumors such as base of skull sarcoma.

- Modern LINACs are able to perform sophisticated techniques:
  - Stereotactic radiosurgery (SRS)
  - Intensity modulated radiotherapy (IMRT)
  - Image-guided radiotherapy (IGRT)

Radiotherapy

- One of the greatest challenges in current radiotherapy is to provide a lethal dose only to a tumor within the tolerance of essential normal tissues. Devices like accelerator-based megavolt x-ray generators, tomotherapy machines, stereotactic radiotherapy systems and intensity modulated radiation therapy systems, are not sufficient to treat cancers because they fail to kill developed metastases outside the targeted volume.

- Use of radiosensitizers could compensate for the insufficiency of equipment-based treatment. Loading with gold nanoparticles (AuNPs) is one of the promising candidates in this area.

Radiotherapy Safety

- Radiotherapy has unique features from the point of view of the potential for accidental exposure
- Consequences of accidental exposure can be very severe and affect many patients
- Careful clinical follow up may detect overdoses from about 10%
- A quality assurance programme is the key element in prevention of accidental exposure

Few examples of RT mistakes

- In June, The Times reported that a Philadelphia hospital gave the wrong radiation dose to more than 90 patients with prostate cancer — and then kept quiet about it. In 2005, a Florida hospital disclosed that 77 brain cancer patients had received 50 percent more radiation than prescribed because one of the most powerful — and supposedly precise — linear accelerators had been programmed incorrectly for nearly a year.
- Dr. John J. Feldmeier, a radiation oncologist at the University of Toledo and a leading authority on the treatment of radiation injuries, estimates that 1 in 20 patients will suffer injuries.
- Even though many accident details are confidential under state law, the records described 621 mistakes from 2001 to 2008. The Times found that on 133 occasions, devices used to shape or modulate radiation beams. On 284 occasions, radiation missed all or part of its intended target or treated the wrong body part entirely. In one case, radioactive seeds intended for a man's cancerous prostate were instead implanted in the base of his penis.

Background

- During the period 1974-1976 the physicist failed to perform regular measurements (calibrations and QA)
- The physicist relied on estimations of the decay of the source to predict dose rate and calculate treatment time
- Rather than calculated decay, the physicist plotted dose rate on graph paper and extrapolated

Impact of accident

- 426 patients received significant overdoses
- 11 were untraced - 415 followed up
- 795 sites at risk identified
- 57% (243) died within the first year
- In 87 patients there was local control with no documented recurrence
- Survivors beyond the second year had an increased frequency of complications

Interaction of radiation with matter

When radiation interacts with matter, a number of processes can result…

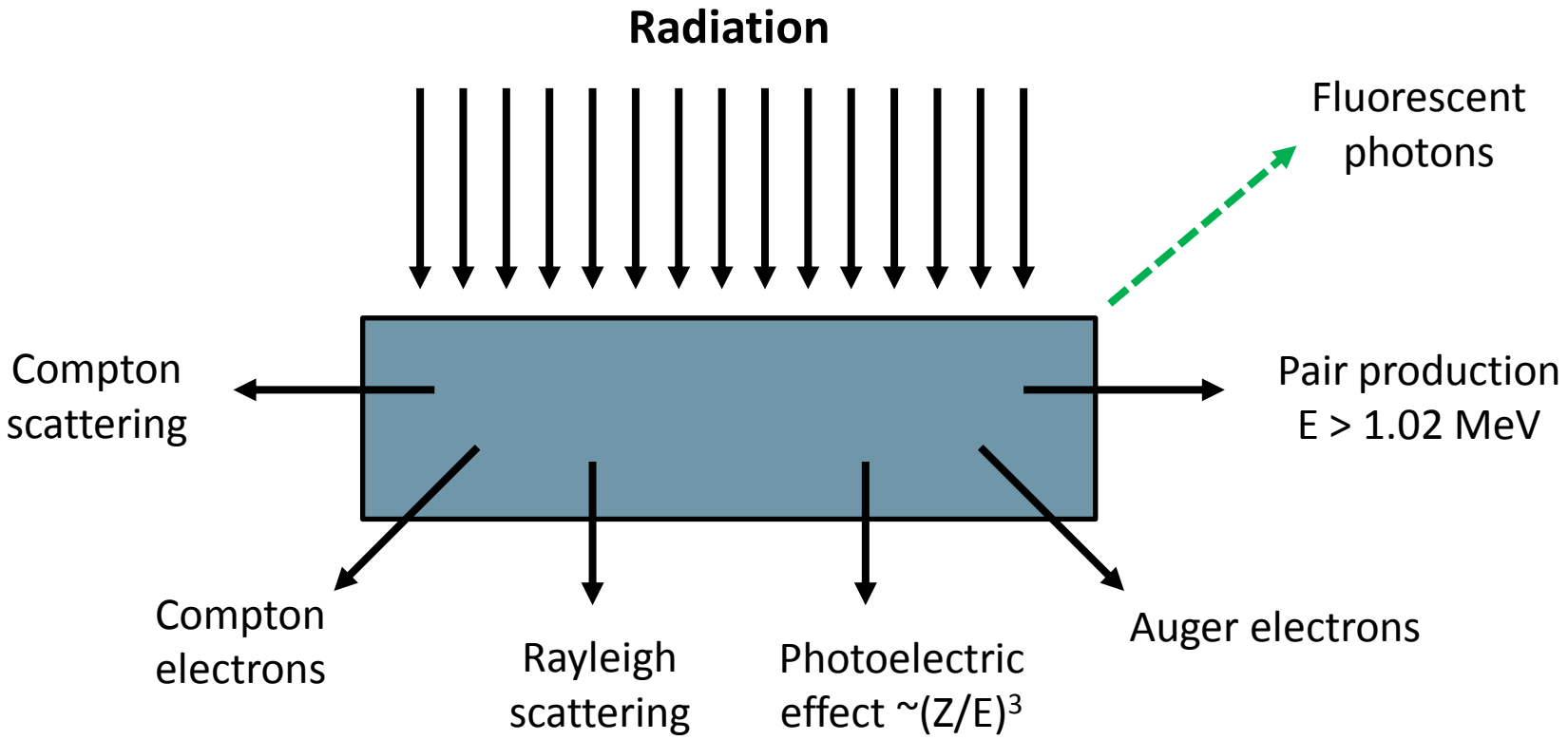

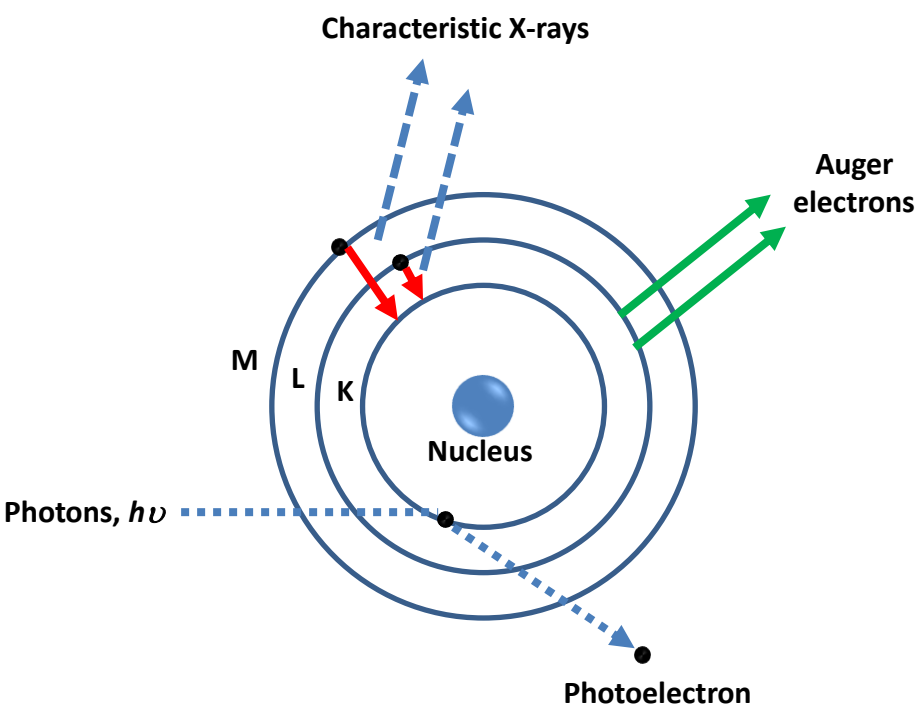
Characteristic X-rays
Auger electrons
M
L
K
Nucleus
Photons, hυ
Photoelectron

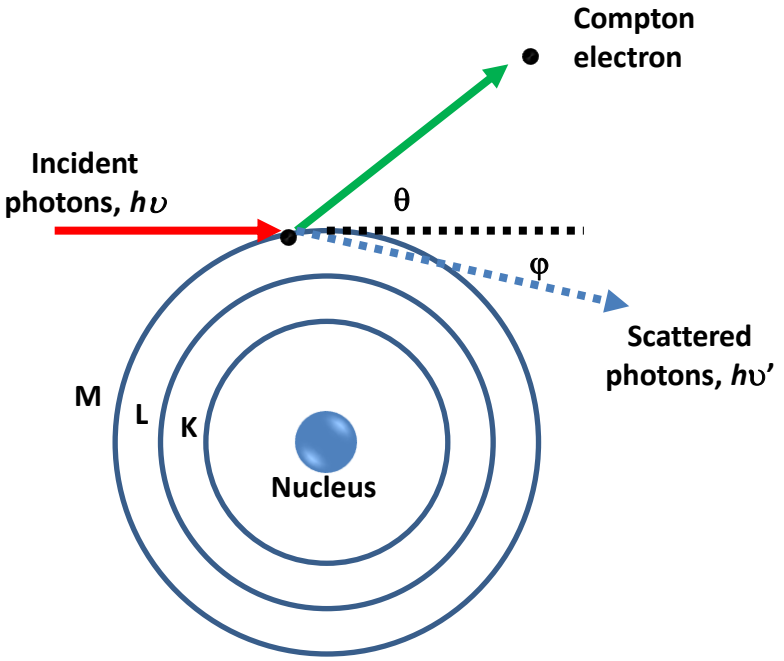
Compton electron
Incident photons, hυ
θ
φ
Scattered photons, hυ'
M
L
K
Nucleus

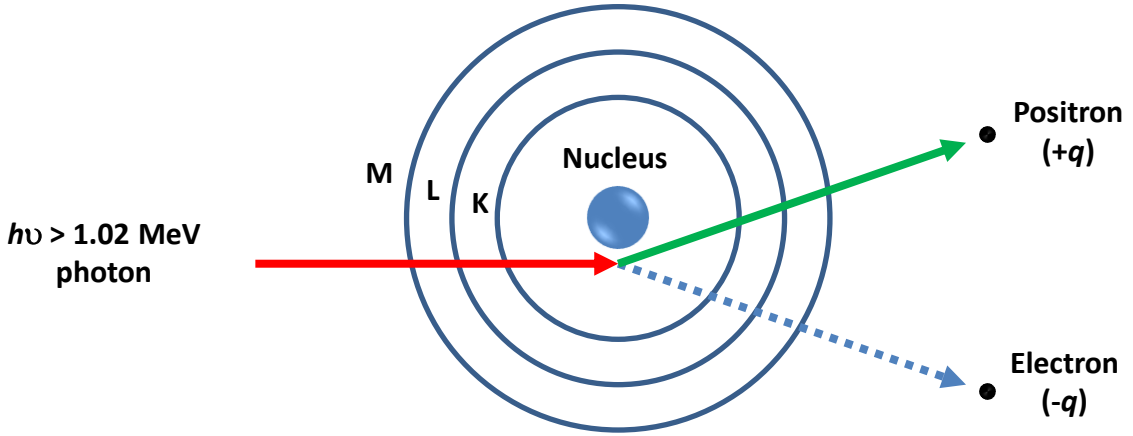
M
L
K
Nucleus
hυ > 1.02 MeV photon
Positron (+q)
Electron (-q)

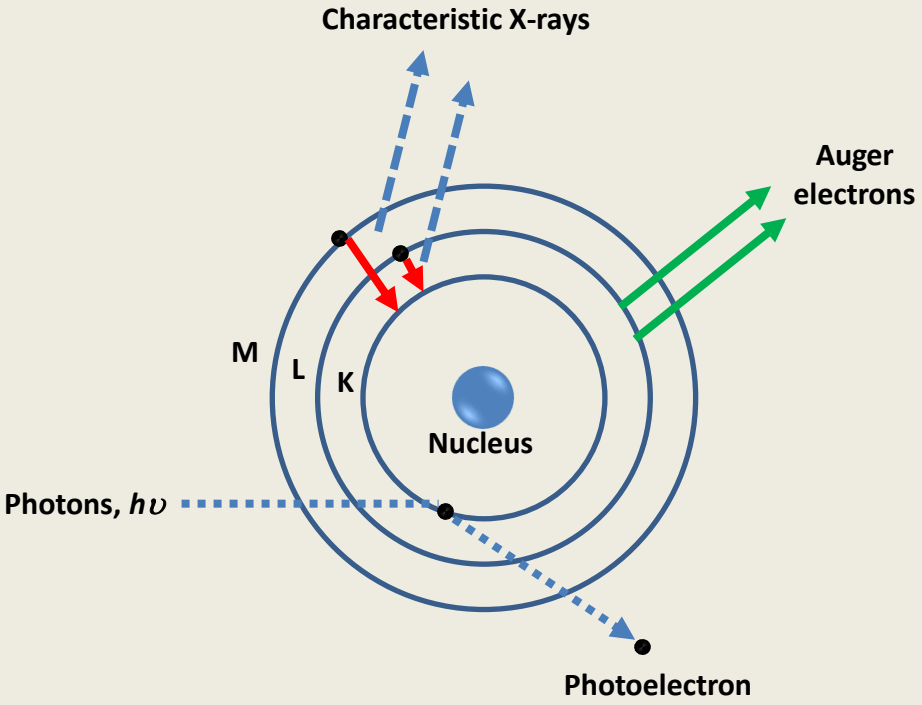

The photoelectric effect:
Ejects inner shell orbital electrons leaving a vacancy in the inner shell which is filled by an electron from an outer orbit releasing a characteristic x-rays. These x-rays are absorbed locally by an orbital electron that will be emitted as Auger electron.

The probability for photoelectric effects is proportional to $(Z/E)^3$. For high Z materials (such as gold) the interaction dominates at energies < 0.5 MeV while for tissues photoelectric effect is dominant at energies below 30 keV.

Biological damage

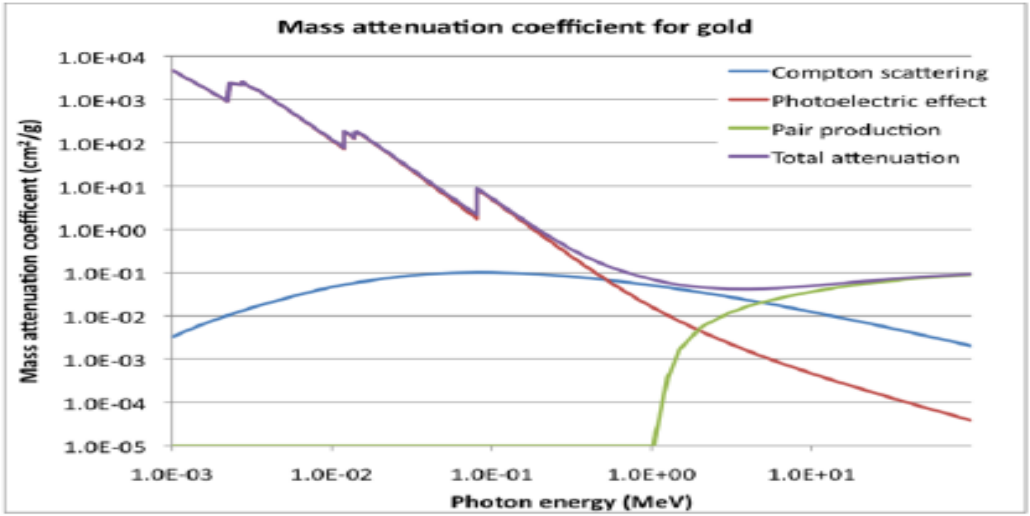

Figure D-1: Mass attenuation coefficients for gold separated by interaction type

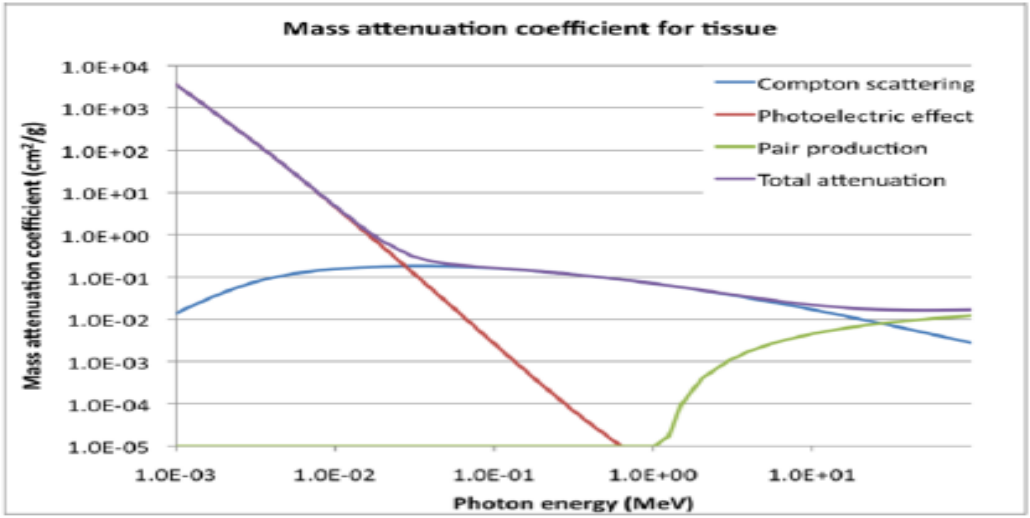

Figure D-2: Mass attenuation coefficients for tissue separated by interaction type

M. Misawa, J. Takahashi / Nanomedicine: Nanotechnology, Biology, and Medicine 7 (2011) 604–614

AuNPs contribute to enhanced generation of reactive oxygen species (ROS) like ·OH, O_2^- , and $^1O_2$ under irradiations of x-rays in the diagnostic range. Enhanced generation of ROS by AuNPs under x-ray irradiation can be explained by the emission of photo- and Auger- electrons and fluorescent x-rays emitted in the interaction of incident x-rays with AuNPs. Generation of ROE may become additional contributors to tumor therapy in a novel photon-activated x-ray radiotherapy.

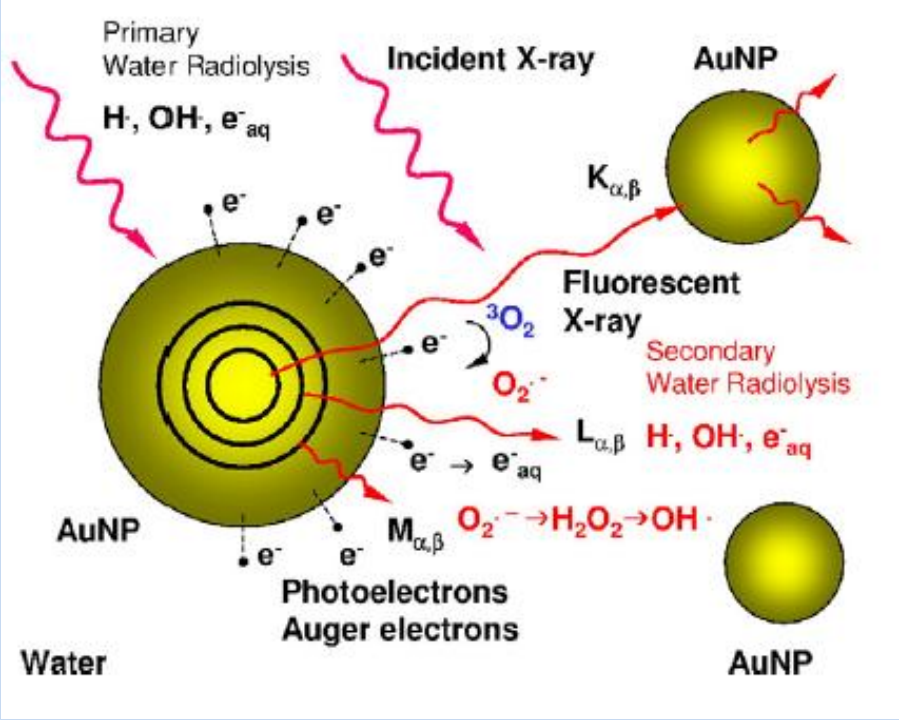

Biological damage

The interaction of ionizing radiation with biological matter result in the production of secondary electrons and free radicals, that will interact with other atoms and produce a chain of biological effects, like single and double strand breaks on DNA.

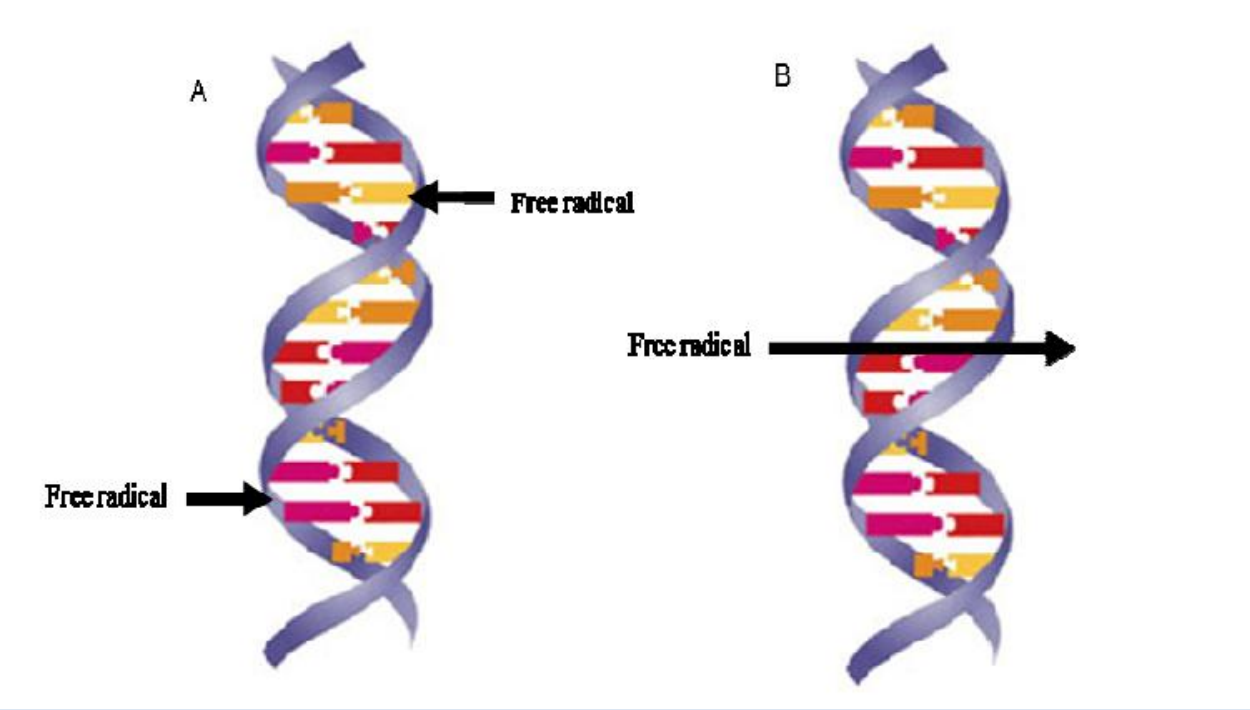

Cell survival curves

- The damage by ionizing radiation to biological matter is usually quantified by using cell survival curves.

- Cell survival curves represent the relationship between the radiation dose and the proportion of cells that survive irradiation as measured *in vitro.*

- The shape of the cell survival curves is dependent on factors such as the type or radiation and the cell line.

- The shape of cell survival curve is usually described using radiobiological models and one of the most common models used is the linear quadratic model (LQ).

Cell survival curves

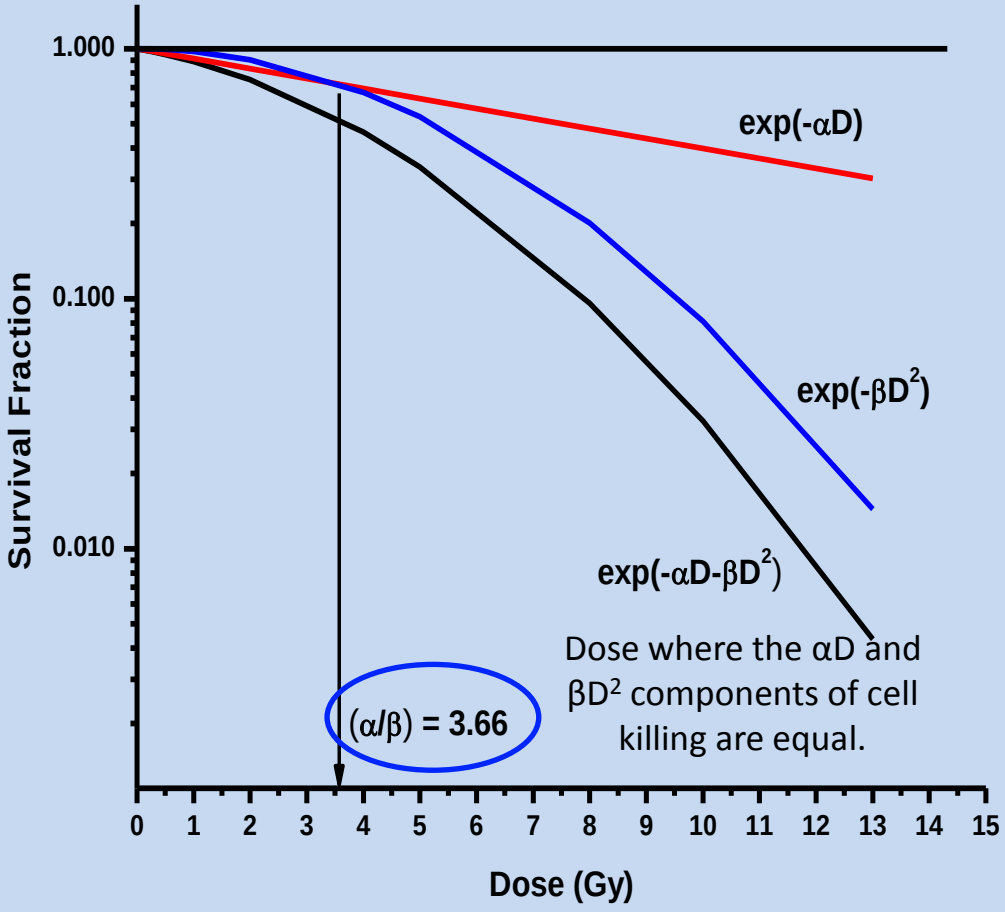

Linear Quadratic Model

$$S = \exp(-\alpha D - \beta D^2)$$

Proportional to the dose

Indicates the probability of an interaction between the two chromosomes breaks

Proportional to the square of the dose

Probability of two separate electrons breaking both of the two chromosomes

Dose enhancement by high-Z materials

- Dose enhancement at interfaces between high and low Z materials has been studied for over 60 years. This effect caused burns and necrosis in tissue around reconstructive wires in mandibular cancer patients after RT.

- Then, Matsudaira et al. measured a radioenhancing effect of iodine contrast agent on cultured cells, demostrating the use of iodine as a radioenhancer in the 80's.

- Since then, there has been a considerable amount of reports of radiation enhancement studies using different materials like contrast agents (iodinated and gadolinium compounds), chemotherapy drugs (cis-platinum) and metallic nanostructures.

Hainfeld, J. F. et al. Phys. Med. Biol. 2004,49: N309-N315
Rahman, W. N. Gold Nanoparticles: Novel Radiobiological Dose Enhancement Studies for Radiation Therapy, Synchrotron based Microbeam and Stereotactic Radiotherapy. Ph. D. Thesis. 2010

Dose enhancement by high-Z materials

- The research in radiation dose enhancing involves the search for materials and radiation sources that help us to improve the radiotherapy without causing (or minimizing) damage to healthy tissue.

- Distinct materials had been used to this goal like gadolinium and iodinated compounds, platinum and recently, **gold nanoparticles**, that is the main material discussed in this talk.

- There is a lot of papers that report Monte Carlo simulations, *in vivo* and *in vitro* assays that try to explain the phenomena and find the best parameters to optimize the dose enhancement effect.

Dose enhancement by high-Z materials

Authors	Year	Conclusions
Matsudaira et al.	1980	The influence of an iodine contrast medium on several responses to radiation was examined in mammalian cells in culture (L5178Y). The presence of the medium at the time of irradiation enhanced cell killing, frequency of micronuclei, and yield of DNA single-strand breaks induced by X rays, depending on the concentration used, whereas no such effect was found with γ rays. It was concluded that the contrast medium sensitizes mammalian cells in culture primarily by means of the photoelectric effect, thereby increasing the absorbed dose of X rays in the cells.
Santos et al.	1983	The authors demonstrated the effect of iodine concentration and radiation quality on the dose enhancement in lymphocytes and calculate the effect of such effect on depth dose distributions in the brain after direct injection into rabbit brains. The combination of low-energy x-ray and contrast media is more effective than the agent alone in causing the regression of mouse tumors.
Iwamoto et al.	1987	Loading tissue with iodine enhances the radiation dose absorbed from low-energy x-rays, as demonstrated by infusing radiographic contrast media into rabbits carrying VX-2 brain tumors and exposed to 15 Gy of 120 kVp x-rays. The dose enhancement was approximately 30% and the survival after tumor detection increased from 3 to 25.5 to 38.5 days for untreated rabbits, treated with radiation alone and radiation plus contrast media, respectively. The repeated infusion of 3.5 g kg^{-1} of body weight did not affect renal function.
Nath et al.	1990	The dependence of iododeoxyuridine (IUdr) radiosensitization on photon energy and dose rate was investigated by irradiating Chinese hamster cells in vitro. The radiosensitization produced by 10^{-5} and 10^{-4} M IUdr for 28 keV photons from I-125, 60 keV photons from Am-241 and 830 keV photons from Ra-226. Radiosensitization factors (RF) were independent of dose rate from 0.3 to 0.73 Gy/h for all cases except for 10^{-4} M IUdR plus Am-241, in which case the RF increased from 2.5 to 3.0. In all cases, the RF decreased significantly as the dose rate was lowered from 0.30 to 0.17 Gy/h. Moreover, at 0.17 Gy/h the RF were essentially the same for all three photon energies. As the dose rate increased from 0.17 to 0.73 Gy/h, the difference between the RF for the three photon energies became larger; RF for Am-241 were higher than those for Ra-226 and I-125.
Rose et al.	1999	This Phase I study was designed to evaluate the computed tomography (CT) scanner as a device for radiation therapy of human brain tumors (CTRx) and to increase the therapeutic radiation dose to tumors compared to normal tissue by concentration of infused contrast material in tumors. None of the patients showed adverse reactions to the CM or necrosis of the normal brain from the CTRx boost radiation. Monte Carlo calculations of the radiation dose distributions in a model tumor showed that the CTRx irradiation of tumors carrying 10 mg of iodine per gram of tumor was as good or better than the dose distribution from conventional 10-MV X-rays. The treated tumor in two of the patients vanished after four treatments, whereas a control tumor in one patient remained constant and grew 4-fold in another patient

Dose enhancement by high-Z materials

Authors	Year	Conclusions
Robar et al.	2002	This study examines the magnitude of tumor dose enhancement achieved by injection of gadolinium or iodine contrast media (CM) and treatment using modified x-ray photon spectra from linear accelerators. Monte Carlo modelling of the linear accelerator and patient geometry was used to explore the effect of removing the flattening filter for various beam qualities and the resultant effect on dose enhancement. Simulation results indicate that for flattened 6–24 MV photon beams and realistic CM tumor concentrations, the dose enhancement remains below 5%. However, if the flattening filter is removed, dose enhancement is increased significantly. For a 30 mg ml^{-1} gadolinium CM tumor concentration, for example, 8.4%, 10.8%, 13.7% and 23.1% dose enhancements are achieved for 18 MV, 6 MV, 4 MV and 2 MV unflattened beams, respectively.
Corde et al.	2004	This study evaluates the optimal X-ray energy for increasing the radiation energy absorbed in tumors loaded with iodinated compounds. SQ20B human cells were irradiated with synchrotron monochromatic beam tuned from 32.8 to 70 keV. Two cell treatments were compared to the control: cells suspended in 10 mg ml^{-1} of iodine radiological contrast agent or cells pre-exposed with 10 mM of IUdr for 48 h. Cells irradiated with both iodine compounds exhibited a radiation sensitization enhancement energy dependent, with a maximum at 50 keV. At this energy, the sensitization calculated at 10% survival was equal to 2.03 for cells suspended in iodinated contrast agent and 2.60 for IUdR. Cells pretreated with IUdR had higher sensitization factors over the energy range than for those suspended in iodine contrast agent. The survival curves presented no shoulder, suggesting complex lethal damages from Auger electrons. These results confirm the optimum energy at 50 keV.
Roeske et al.	2007	Materials with atomic numbers (Z) ranging from 25 to 90 are considered in this analysis and the energy spectrum for a number of external beam x-ray sources and common radionuclides are evaluated. For a nanoparticle concentration of 5 mg/ml, the DEF is < 1.05 for Co-60, Ir-192, Au-198, Cs-137, 6, 18, and 25 MV x-rays for all materials considered. However, relatively large increases in the DEF are observed for 50, 80, 100, and 140 KVp x-rays as well as Pd-103 and I-125. The DEF increases for all sources as Z varies from 25-35. From Z = 40-60, the DEF plateaus or slightly decreases. For higher Z materials (Z>70), the DEF increases and is a maximum for the highest Z materials. High atomic number nanoparticles coupled with low energy external beam x-rays or brachytherapy sources offer the potential of significantly enhancing the delivered dose.
Prezado et al.	2009	In this work, the dose enhancement factors and the peak to valley dose ratios (PVDRs) are assessed for different gadolinium (*Z*=64) concentrations in the tumor and different microbeam energies by using Monte Carlo simulations. A significant decrease in the PVDR values in the tumor, and therefore a relevant increase in the dose deposition, is found in the presence of gadolinium. The optimum energy for the dose deposition in the tumor while keeping a high PVDR in the healthy tissues, which guaranties their sparing, has been investigated.
Townley et al.	2012	The authors report significant and controlled cell death using novel x-ray-activatable titania nanoparticles (NPs) doped with lanthanides. Preferential incorporation of such materials into tumor tissue can enhance the effect of radiation therapy. Herein, the incorporation of gadolinium into the NPs is designed to optimize localized energy absorption from a conventional medical x-ray. This result is further optimized by the addition of other rare earth elements. Upon irradiation, energy is transferred to the titania crystal structure, resulting in the generation of reactive oxygen species (ROS).

Gold nanoparticles

- Among the great variety of nanoparticle-based inorganic systems for biomedical applications, gold nanoparticles play an important role in cancer therapeutics.

- A great variety of these nanostructures had been used like:
  - Spherical nanoparticles
  - Nanorods
  - Nanocages
  - Nanoshells
  - Hollow gold nanospheres

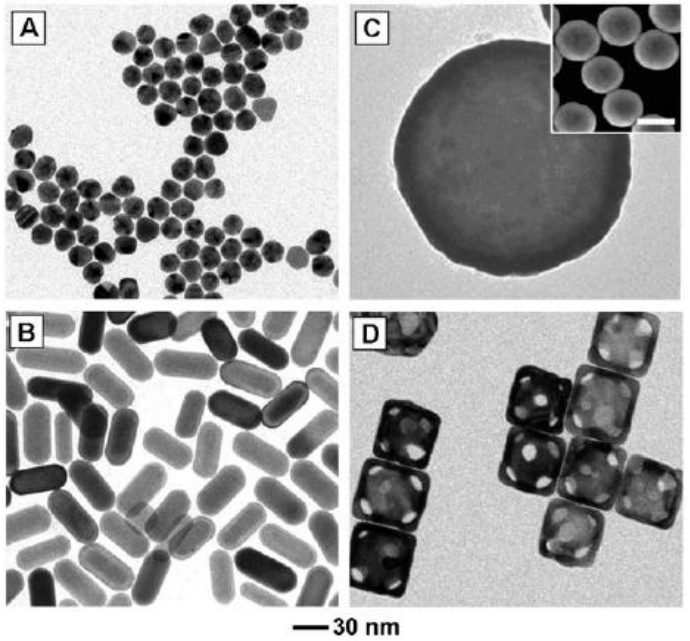

Lim, Z. Z. J. et al. *Acta Pharmacol. Sin.* 2011, 32: 983-990.
Jelveh, S. et al. *Cancers* 2011,3:1081-1110
Cobley, C. M. et al. *Chem. Soc. Rev.* 2011,40:44-56

Gold nanoparticles

- These systems are highly effective platforms for theranostics agent, and have potential to:
  - Drug delivey
  - Cancer diagnostics
  - Photothermal and photodynamic therapy
  - Radiotherapy

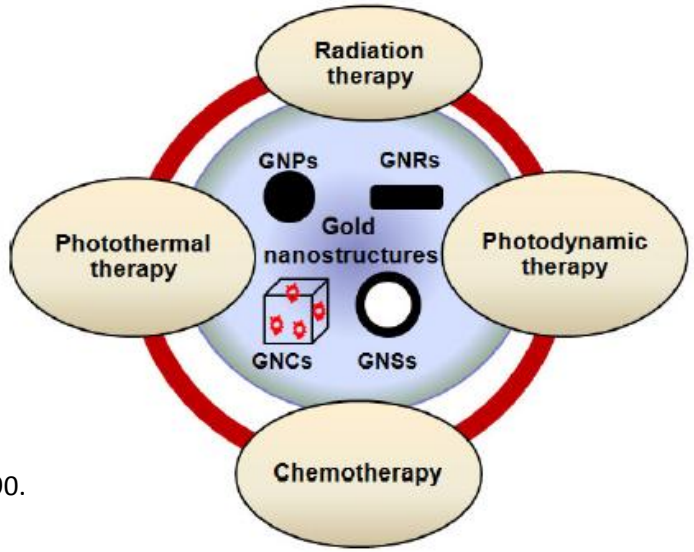

Lim, Z. Z. J. et al. *Acta Pharmacol. Sin.* 2011, 32: 983-990.
Jelveh, S. et al. *Cancers* 2011,3:1081-1110
Cobley, C. M. et al. *Chem. Soc. Rev.* 2011,40:44-56

Why to use gold nanoparticles?

The use of GNPs for biomedical applications is gaining popularity due to several reasons, mainly:

- Gold is considered to be relatively inert and therefore suitable for biomedical applications.
- Strong optical properties.
- Easily controllable surface chemistry, allowing flexible design and multifunctionality.
- Control over particle size and shape during synthesis.
- Gold absorbs ~3-times more than iodine at 20 and 100 keV.

Lim, Z. Z. J. et al. Gold nanoparticles in cancer therapy. *Acta Pharmacol. Sin.* 2011, 32: 983-990.
Hainfeld, J. F. et al. *J. Pharm. Pharmacol*. 2008,60: 970-985

Enhanced Permeability and Retention Effect

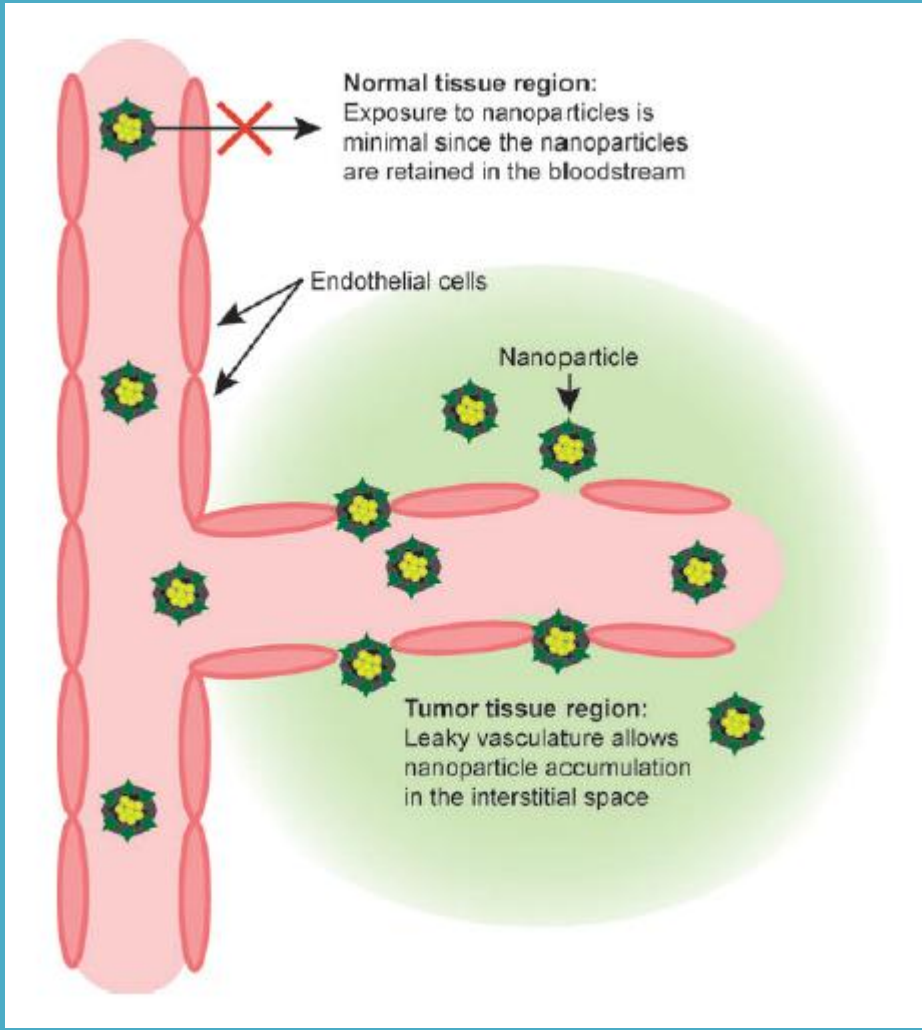

Rapid vascularization in fast-growing cancerous tissues is known to result in leaky, defective architecture and impaired lymphatic drainage. This structure allows an EPR effect, resulting in the accumulation of nanoparticles at the tumor site.

Nie, S. et al. Annu. Rev. Biomed. Eng. 2007, 9: 12.1-12,32

Taking advantage of retention

A. Tumorous tissues suffer of Enhanced Permeability and Retention effect.

B. Nanoparticles injected in the blood stream do not permeate through healthy tissues.

C. Blood vessels in the surrounding of tumorous tissues are defective and porous.

D. Nanoparticles injected in the blood permeate through blood vessels toward tumorous tissues, wherein they accumulate.

Monte Carlo simulations

Many preclinical studies have demonstrated gold nanoparticle (GNP) sensitization with kilovoltage radiation therapy. Monte Carlo modelling of GNP physical dose enhancement predicts sensitization at kilovoltage X-ray energies but not at clinically relevant megavoltage energies.

Monte Carlo simulations

Cho, S. (2005)

Based on the results of Hainfeld et al. (2004) simulated the dose enhancing using a modified phantom and tumor composition defined by ICRU to incorporate different concentrations of GNPs and compared 3 radiation sources.

Concentration (per gram of tumour)	140 kVp	6 MV FF	6 MV NFF	4 MV FF	4 MV NFF
7 mg Au	2.114	1.007	1.014	1.009	1.019
18 mg Au	3.811	1.015	1.032	1.019	1.044
30 mg Au	5.601	1.025	1.053	1.032	1.074

FF: flattening filter, NFF: no flattening filter.

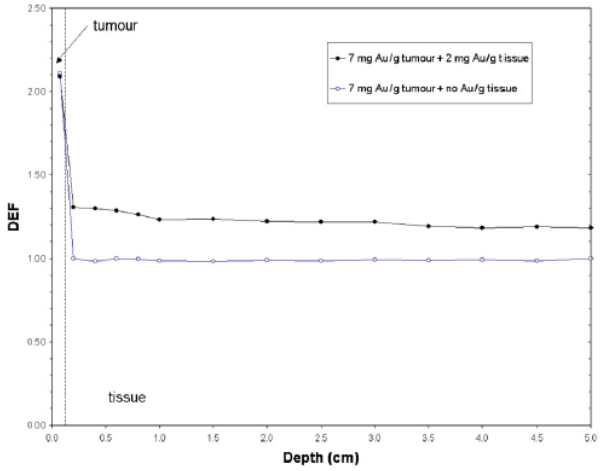

Effect outside the tumor for 140 kVp

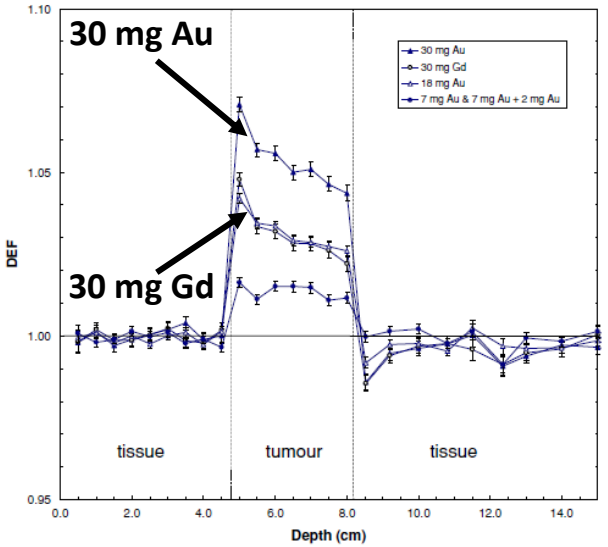

DEF for 6 MV NFF

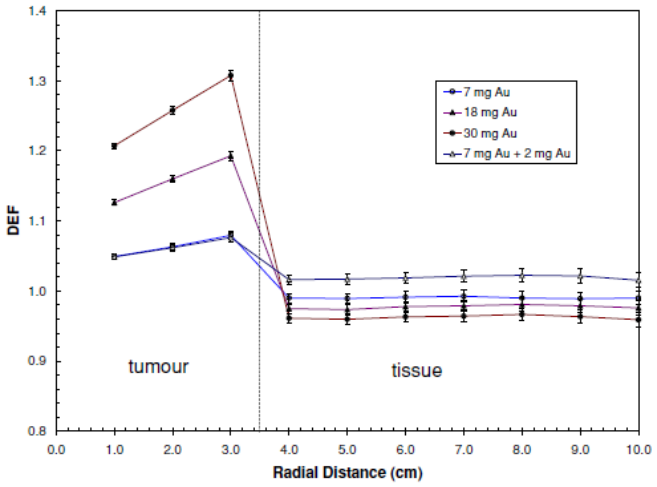

Ir-192 brachytherapy source

Cho, S. H. Phys. Med. Biol. 2005,50: N163-N173

Monte Carlo simulations

McMahon et al. (2008)

As a final test, they used a section from the neck of the Zubal phantom, inserted a tumor and imported into GEANT4

Proposed a figure of merit which enable the direct comparison of diff
different depths inside the patient. The evaluation of the figure o
LINAC and two 150 kVp sources using GNP concentration of 10 mg m

Isodose plots were generated for each of the three types of spectrum, simulating 3 x 10^7 primary events for each source.

Dose volume histograms produced from isodose plots in presence of gold

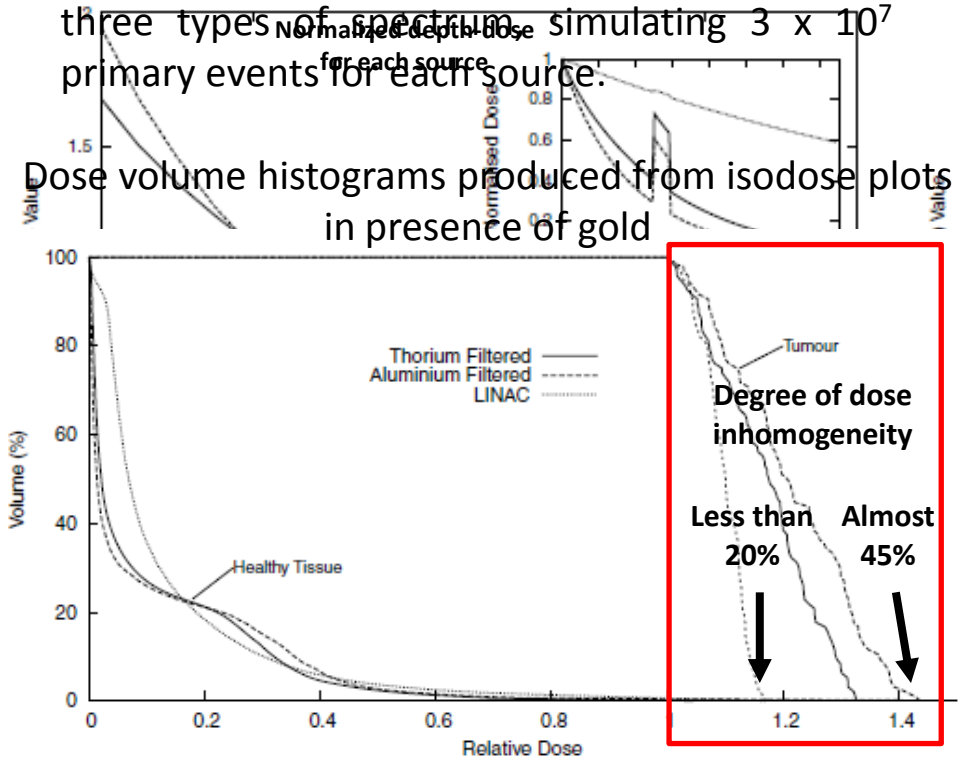

gure of merit ca

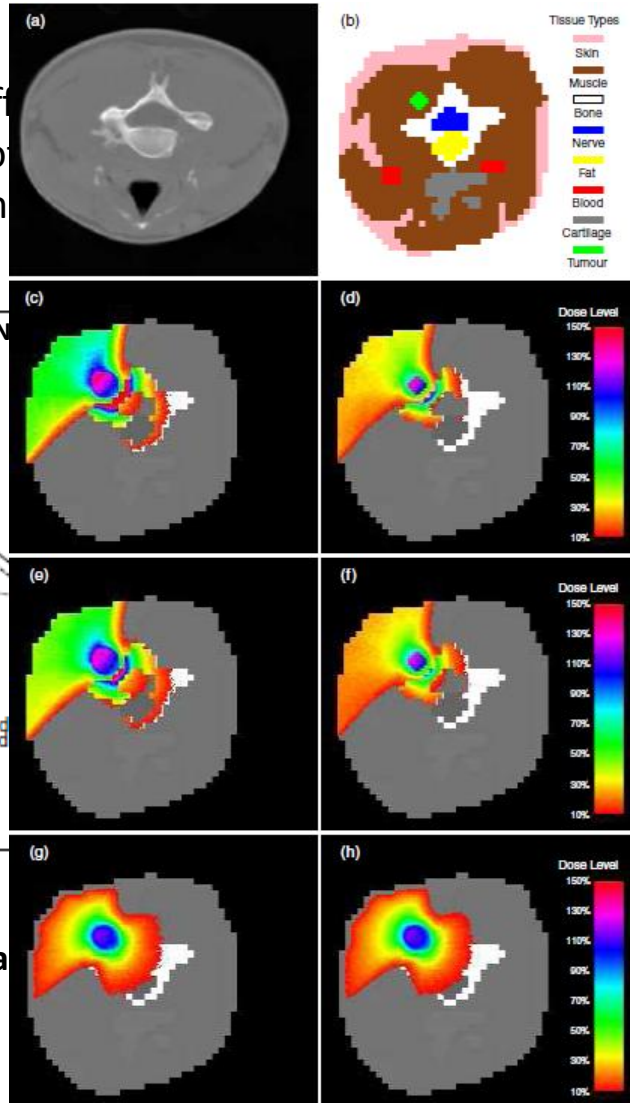

McMahon, S. J. et al. Phys. Med. Biol. 2008,53: 5635-5651

Monte Carlo simulations

Cho, S. (2009)

Photo/Auger electron spectra

Monte Carlo were performed to determine the macroscopic dose enhancement factors (MDEF) during the irradiation of the tumor with different sources with E_{avg} <100 keV. And the photo/Auger electron spectra within a tumor loaded with GNP.

The spectra show a remarkable change in the photoelectron fluence and energy due to the presence of GNP.

Similar pattern of increase in photoelectrons fluence, the difference is below 20 keV, due to increased photon interactions around L- and M- photoelectric absorption edges

The photoelectron contribute to the local energy deposition significantly more (a factor of ~3) than the Auger electrons, even though the fluence is comparable

The fall-off was more pronounced for the 50 kVp and I-125 than for Yb-169 and it is proportional to GNP concentration within a tumor

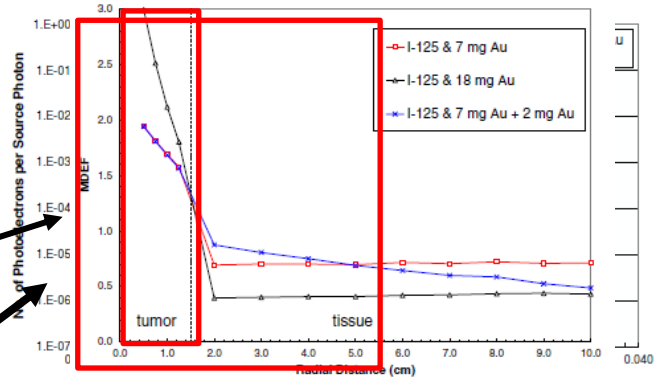

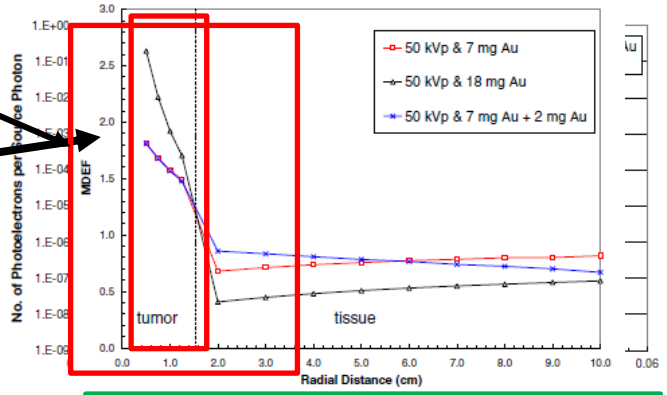

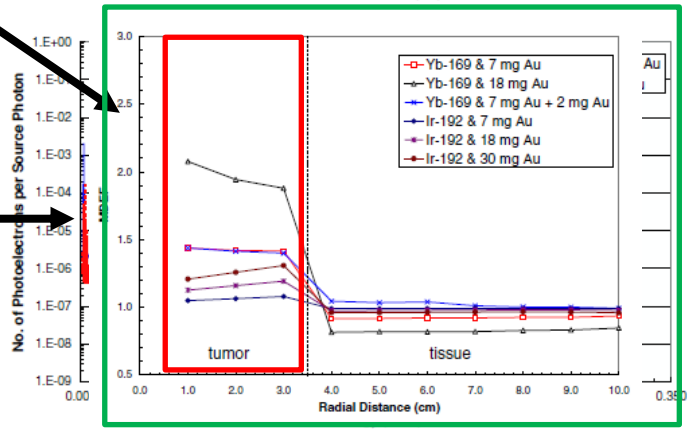

Source	Total PE Fluence gold	Total PE Energy (keV) gold	Total PE Fluence tissue	Total PE Energy (keV) tissue	Total PE Energy (keV)	Total AE Fluence gold	Total AE Energy (keV)
^{125}I	0.337	5.28	0.132	7.24	12.5	0.622	2.25
50 kVp	0.307	4.84	0.311	6.62	11.5	0.569	2.07
^{169}Yb	0.068	2.85	0.048	1.76	4.61	0.126	0.47

Comparison of MDEF between Yb-169 and Ir-192

Yb-169 > Ir-192

Cho, S. H. et al. Phys. Med. Biol. 2009,54: 4889-4905

Monte Carlo simulations

Montenegro et al. (2009)

They assumed normal body material embedded with GNP to demostrate that resonant excitations, transitions result in a considerable enhancement in localized X-ray energy deposition and consequently in the processes and energies

Large number of electron emitted correlated to the large energy absorption

A similar situation occur with the emission of photons in the tumor region

Consistent with its larger number of photons reaching the tumor, the 2 MeV beam produce more electrons than 82 keV photons

The presence of GNPs has increased the energy deposited at the tumor by more than 25 times that at 82 keV

The introduction of GNP has a marginal effect for the 2 MeV beam due to the small photoelectric cross section

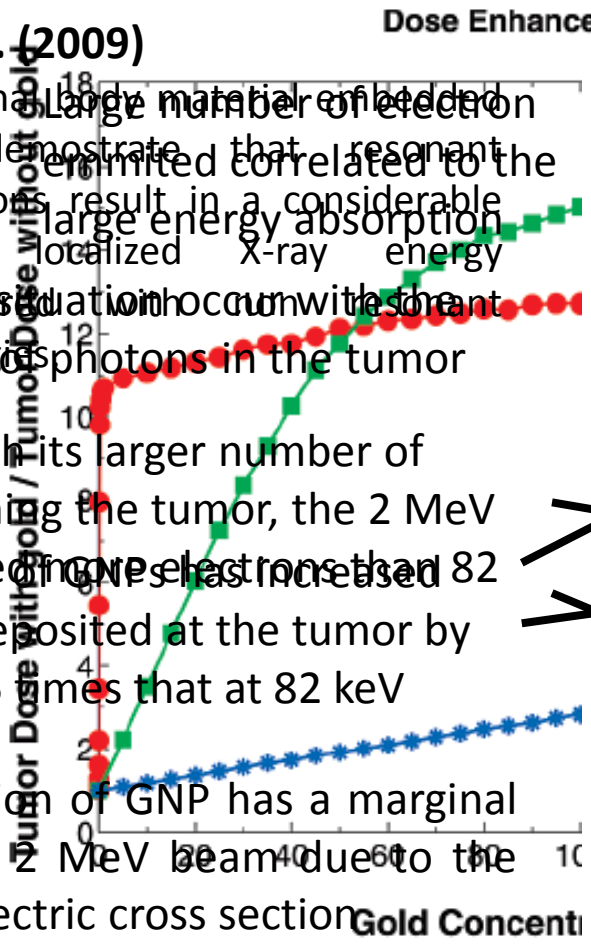

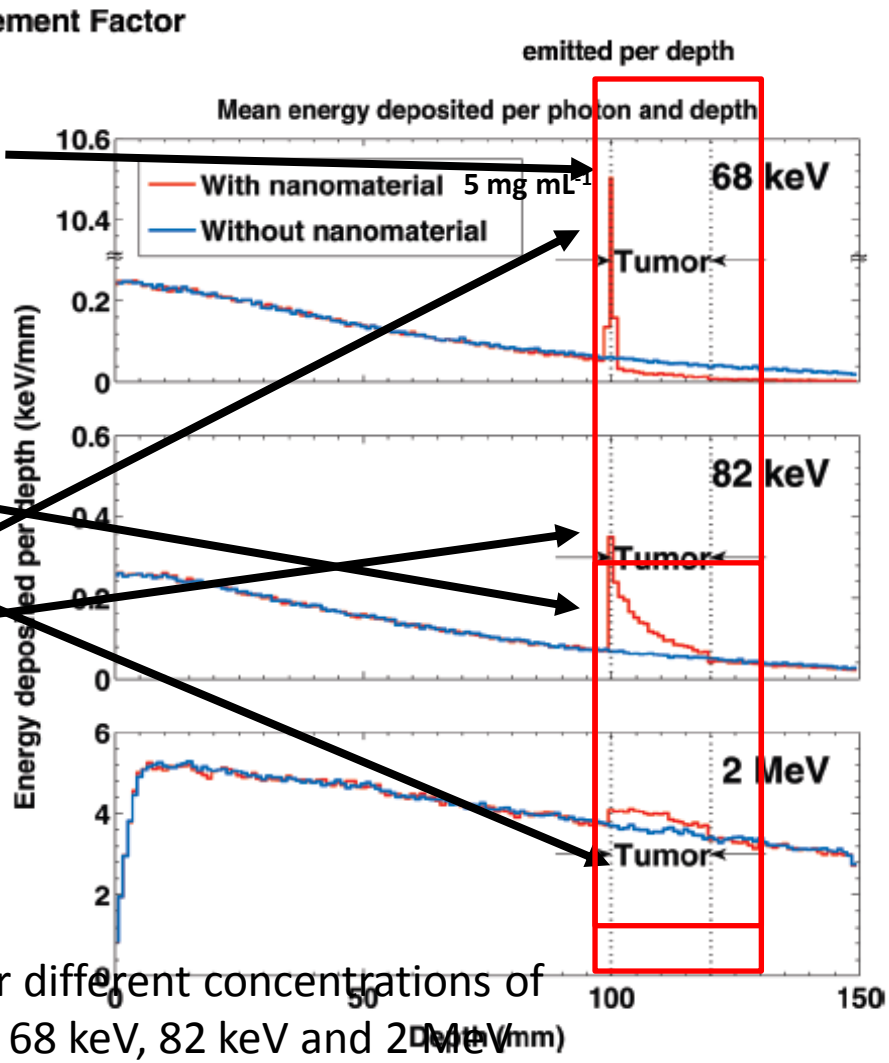

Dose enhancing factors (DEF) for different concentrations of GNPs and three energy beams 68 keV, 82 keV and 2 MeV

Montenegro, M. et al. J. Phys. Chem. A 2009,113: 12364-12369

Monte Carlo simulations

Ngwa et al. (2010)

In this study, the potential for applying GNPs as vascular disrupting agents is examined and analytical calculations based on electron energy loss formula by Cole were carried out to estimate the endothelial dose enhancement caused by radiation-induced photo/Auger electrons originating from GNPs targeting the tumor endothelium.

EDEF due to photoelectrons

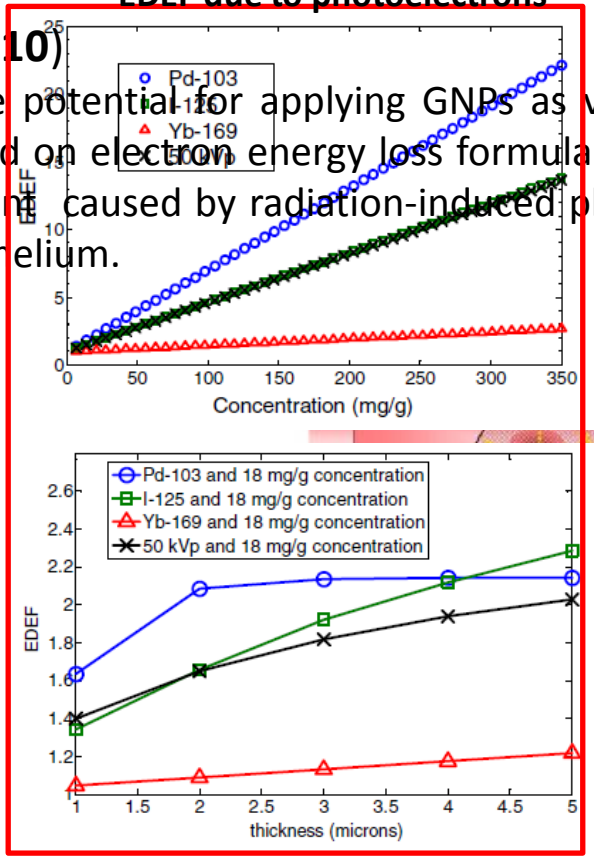

EDEF due to Auger electrons

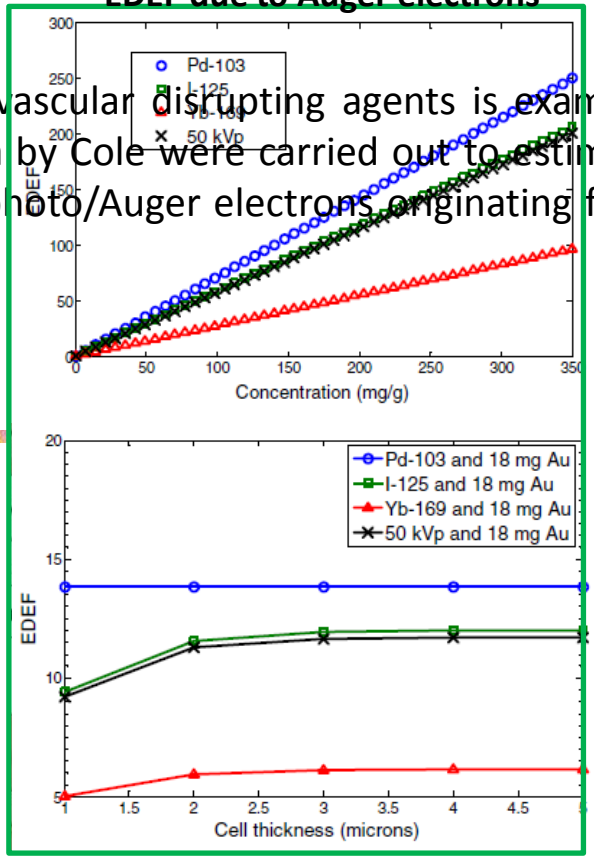

	EDEF due to photoelectrons			EDEF due to Auger electrons			Total EDEF		
	7 mg g^{-1}	18 mg g^{-1}	350 mg g^{-1}	7 mg g^{-1}	18 mg g^{-1}	350 mg g^{-1}	7 mg g^{-1}	18 mg g^{-1}	350 mg g^{-1}
Pd-103	1.42	2.09	22.15	5.99	13.82	250.33	7.41	15.91	271.48
I-125	1.26	1.66	13.79	5.10	11.55	206.12	6.36	13.21	219.91
Yb-169	1.03	1.09	2.71	2.92	5.93	96.95	3.95	7.02	99.66
50 kVp	1.25	1.65	13.63	5.00	11.28	200.83	6.25	12.93	214.46

Ngwa, W. et al. Phys. Med. Biol. 2010,55: 6533-6548

Monte Carlo simulations

D
L
I
c
c
a

Table 3. Ratio of mean energy over mean range of escaping electrons (keV μm^{-1}).

	Photon source							
	Pd-103				I-125			
AuNP diameter (nm)	1.9	5	30	100	1.9	5	30	100
Auger and delta electrons	8.54	8.46	7.73	7.50	8.56	8.50	7.74	7.48
Photoelectrons	4.77	4.78	4.82	4.82	3.62	3.62	3.64	3.70
All electrons	7.47	7.39	6.61	6.16	7.18	7.10	6.16	5.50
	Yb-169				300 kVp			
AuNP diameter (nm)	1.9	5	30	100	1.9	5	30	100
Auger and delta electrons	7.00	6.89	6.10	5.61	4.63	4.58	4.02	3.56
Photoelectrons	1.55	1.55	1.55	1.55	1.23	1.23	1.23	1.23
All electrons	5.52	5.39	4.38	3.50	3.69	3.63	2.98	2.38
	Ir-192				6 MV			
AuNP diameter (nm)	1.9	5	30	100	1.9	5	30	100
Auger and delta electrons	4.74	4.67	4.13	3.63	5.60	5.56	4.85	4.28
Photoelectrons	0.67	0.67	0.67	0.67	0.50	0.49	0.49	0.49
All electrons	3.61	3.54	2.81	2.10	4.12	4.07	3.18	2.35

Auger electrons | Photoelectrons | Characteristic x-rays | Internaly absorbed

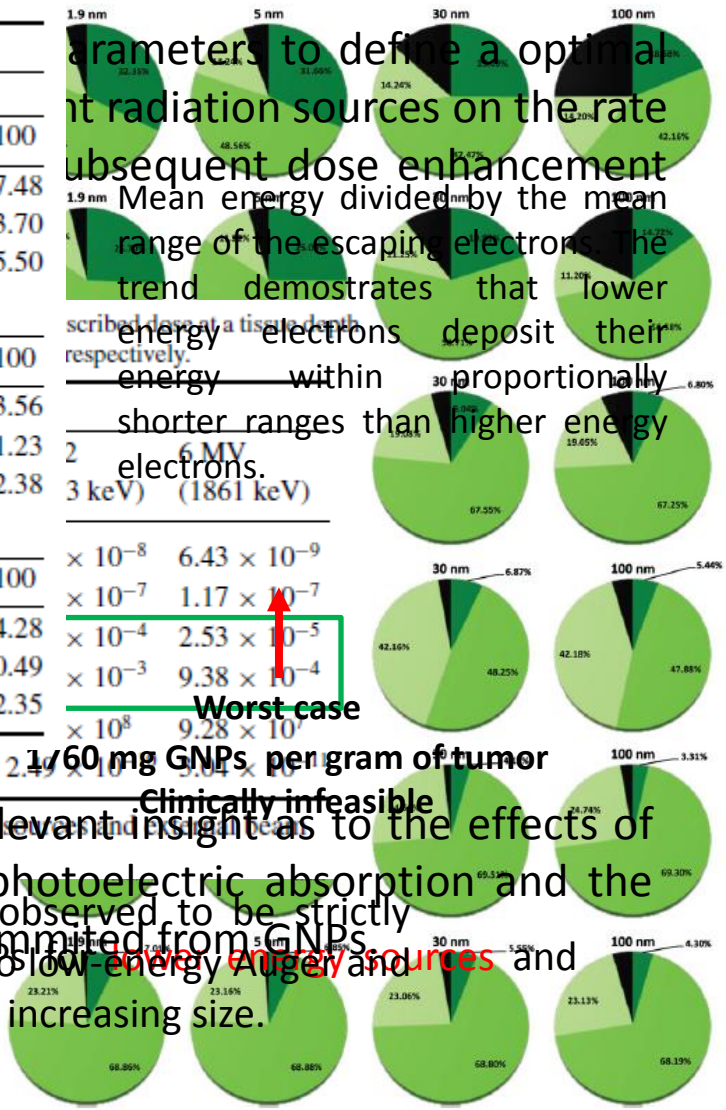

arameters to define a optimal
nt radiation sources on the rate
ubsequent dose enhancement

Mean energy divided by the mean range of the escaping electrons. The trend demostrates that lower energy electrons deposit their energy within proportionally shorter ranges than higher energy electrons.

scribed here at a tissue depth
respectively.

2 6 MV
3 keV) (1861 keV)

	$\times 10^{-8}$	6.43×10^{-9}
	$\times 10^{-7}$	1.17×10^{-7}
	$\times 10^{-4}$	2.53×10^{-5}
	$\times 10^{-3}$	9.38×10^{-4}
	$\times 10^{8}$	9.28×10^{7}
Per Au atom	3.48×10^{-8}	3.05×10^{-8}	6.06×10^{-9}	3.60×10^{-9}	2.49×10^{-9}	3.04×10^{-9}

sources, respectively.

ionizations.

The results presented in this study provide clinically relevant insight as to the effects of photon source energy and GNPs size on the rate of photoelectric absorption and the subsequent spatial distribution of secondary radiation emmited from GNPs.

Dose enhancement as a function of GNP size was not observed to be strictly proportional to GNP radius cubed. This can be attributed to low-energy Auger and delta electrons being absorbed more readily within GNP of increasing size.

Lechtman, E. et al. Phys. Med. Biol. 2011,56: 4631-4647

In vitro studies

In vitro studies

Herold et al. (2000)

They investigated dose enhancement and radiosensitization associated with electrons produced and scattered from gold microspheres suspended in cells *in vitro* irradiated with kilovoltage x-ray photons

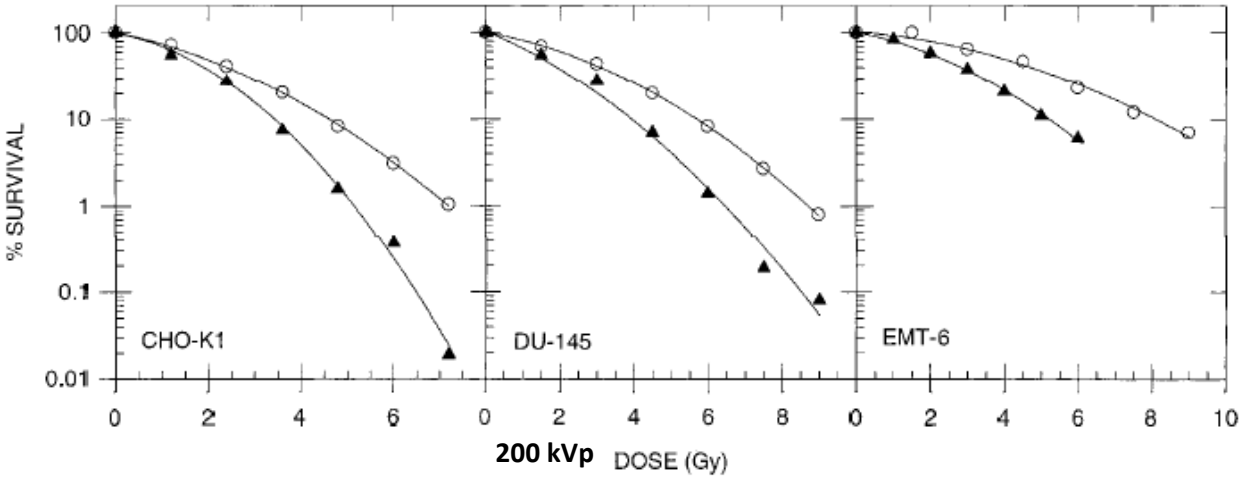

Cell lines	Control (no gold) α (Gy^{-1})	Control (no gold) β (Gy^{-2})	1% Gold α (Gy^{-1})	1% Gold β (Gy^{-2})	DMF at % survival 50%	10%	1%
CHO-K1	0.233 ± 0.04	0.0569 ± 0.006	0.3046 ± 0.05	0.111 ± 0.01	1.36	1.38	1.38
EMT-6	0.092 ± 0.056	0.0251 ± 0.006	0.1932 ± 0.03	0.051 ± 0.005	1.64	1.54	1.50
DU-145	0.158 ± 0.017	0.0426 ± 0.002	0.2593 ± 0.08	0.681 ± 0.012	1.48	1.43	1.33

1.43 Overall DMF

DEF 1% Au
1.42

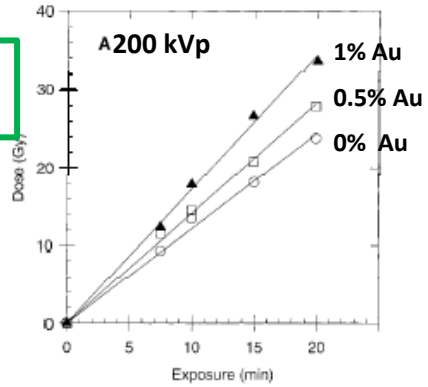

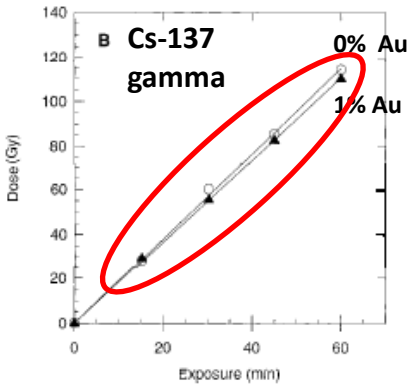

Fricke Dosimeter

Herold, D. M. et al. Int. J. Radiat. Biol. 2000, 76: 1357-1364

In vitro studies

Chien et al. (2007)

They synthesized 20 nm GNP by a synchrotron x-ray method and incubated CT-26 cells with it for 24h, subsequently they irradiated with electron from a linear accelerator with a beam energy of 6 MeV at various doses in a single fraction.

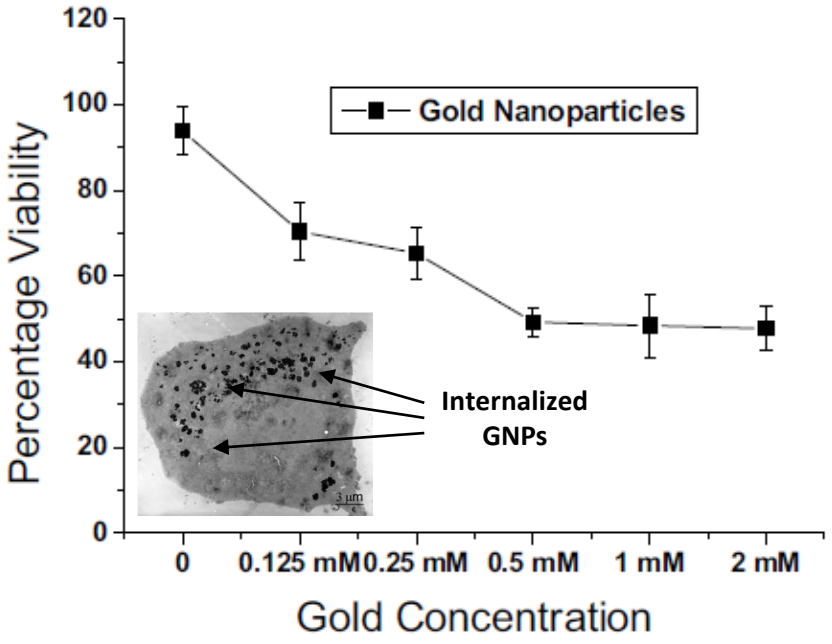

The GNPs tested in this report showed the cytotoxicity depended on the concentration of GNPs

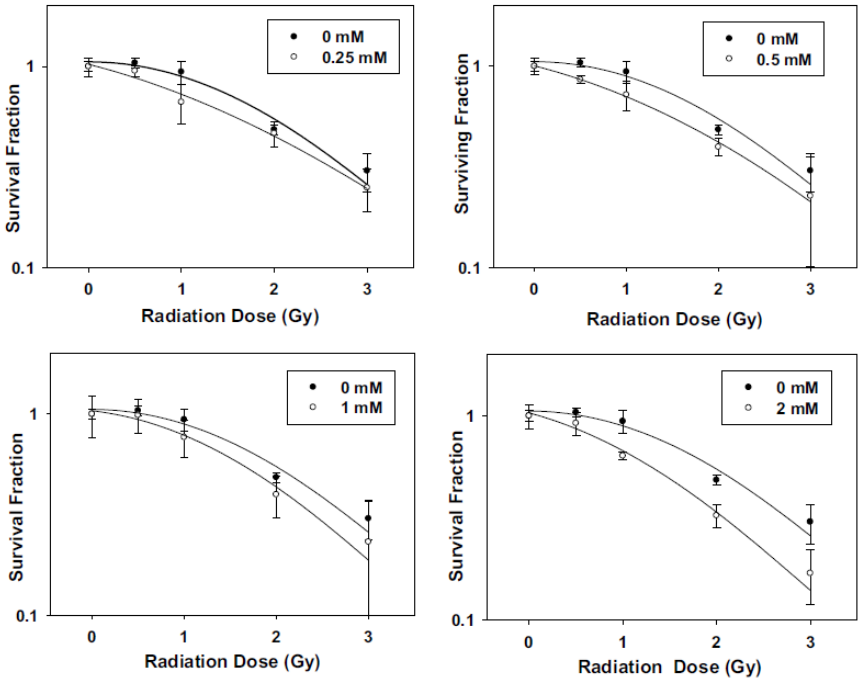

The enhanced cell inhibition was more pronounced at higher radiation doses

Chien, C. C. et al. AIP Conf. Proc. 2007, 879: 1908-1911

In vitro studies

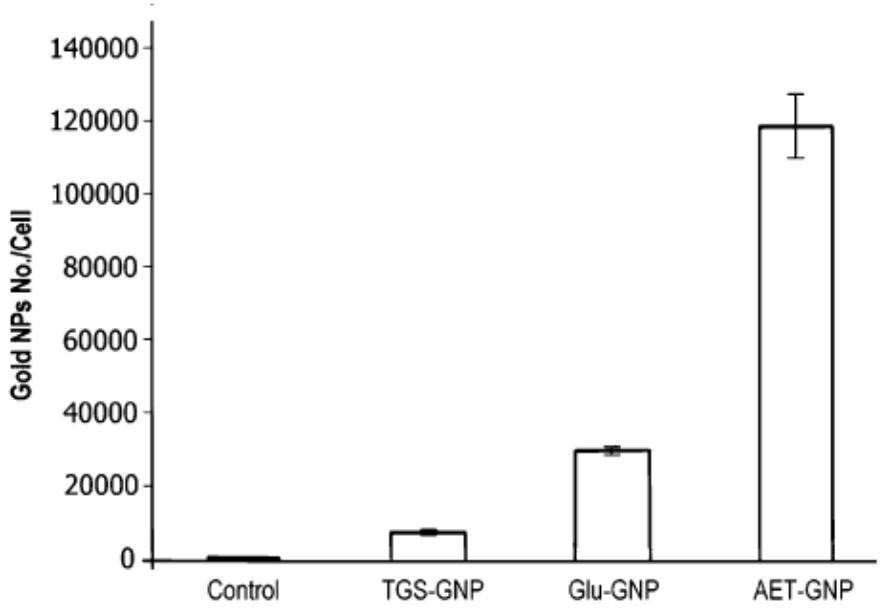

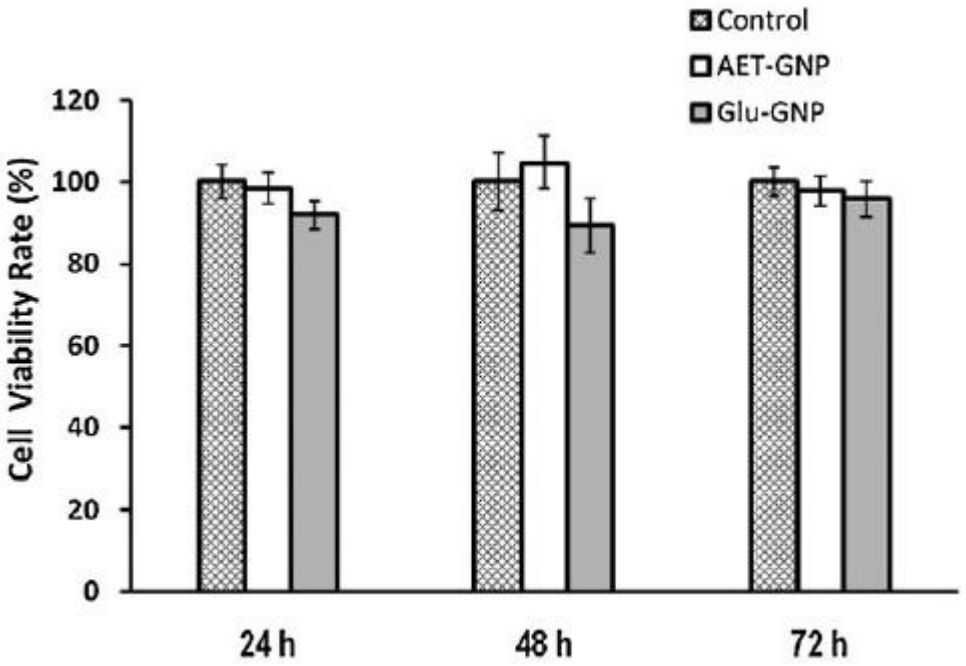

Cell uptake of GNPs

Toxicity test

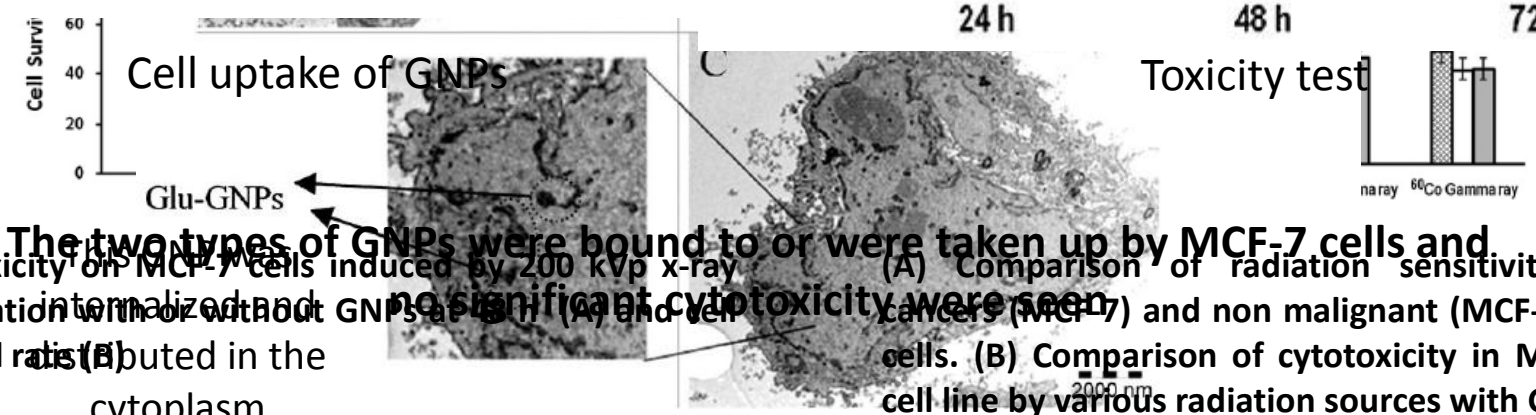

The two types of GNPs were bound to or were taken up by MCF-7 cells and no significant cytotoxicity were seen

Cytotoxicity on MCF-7 cells induced by 200 kVp x-ray irrdadiation with or without GNPs at 5 h (A) and cell survival ratio (B)

(A) Comparison of radiation sensitivity in cancers (MCF-7) and non malignant (MCF-10A) cells. (B) Comparison of cytotoxicity in MCF-7 cell line by various radiation sources with GNPs

- TEM images showed that GNPs were internalized and distributed in the cytoplasm

Kong, T. et al. Small 2008, 4: 1537-1543

In vitro studies

Zhang et al. (2008)

GNPs enhance radiation cytotoxicity

In this s… …ty and growth … …J-145). They ex… …ibition rate.

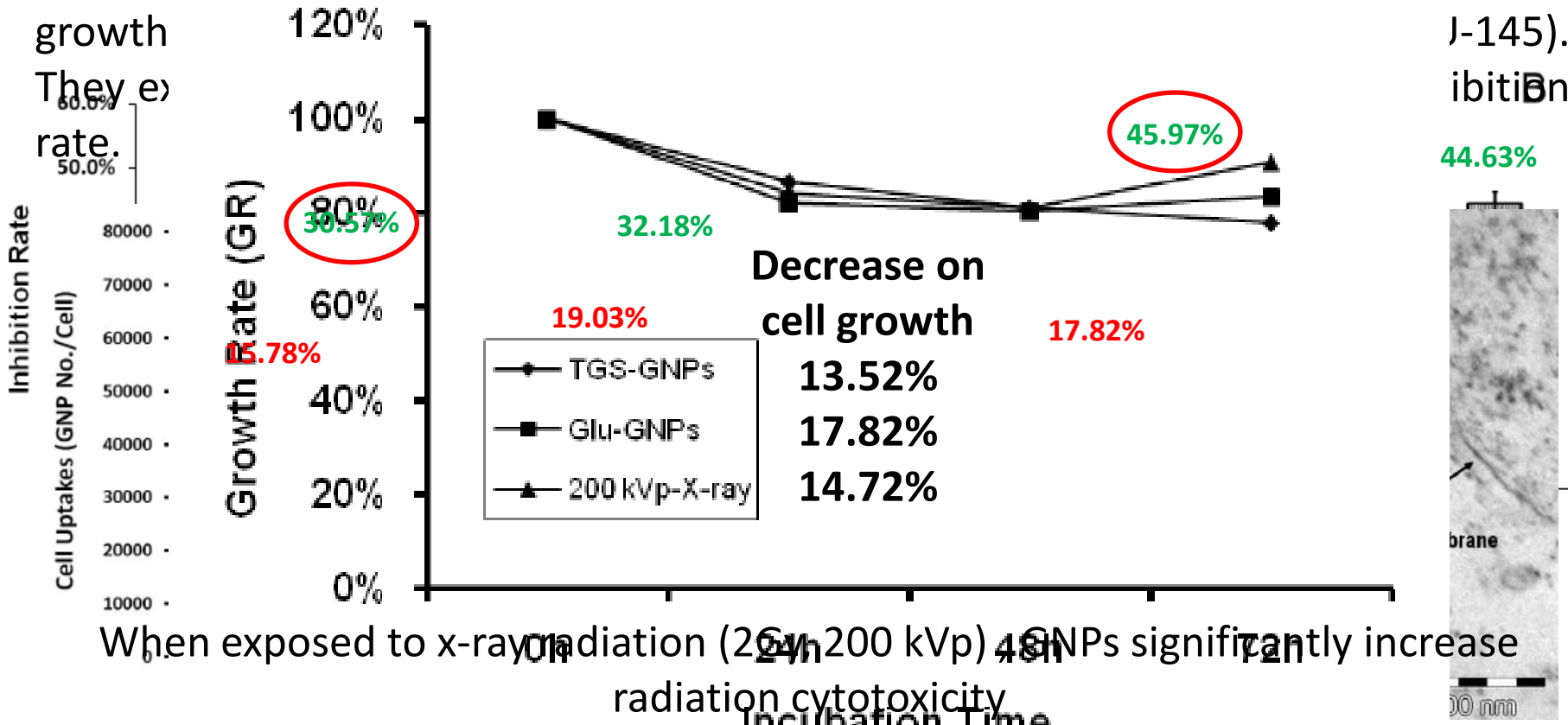

When exposed to x-ray radiation (2Gy, 200 kVp) GNPs significantly increase radiation cytotoxicity

Glucose help to deliver GNPs into cells more efficiently

Cell growth was not different after exposure to TGS-GNPs, Glu-GNPs or x-ray treatment

…s uniformly distributed in the cytoplasm compared to naked GNPs

Zhang, X. et al. Clin. Invest. Med. 2008, 31: E160-E167

In vitro studies

Dose Enhancement

Rahman et al. (2009)

In this work GNPs have been used for enhancement of radiation effects on bovine aortic endothelial cells (BAEC) of superficial x-ray therapy and megavoltage electron radiation therapy beams.

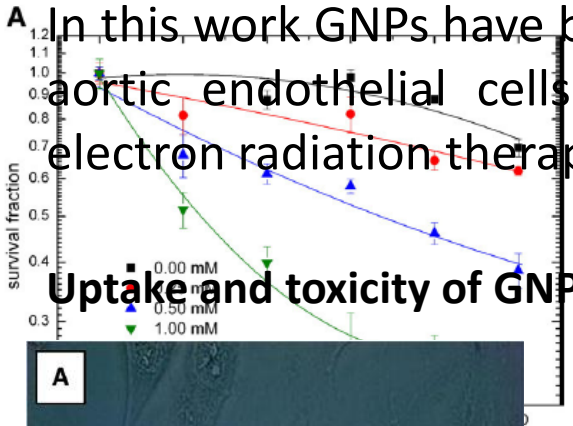

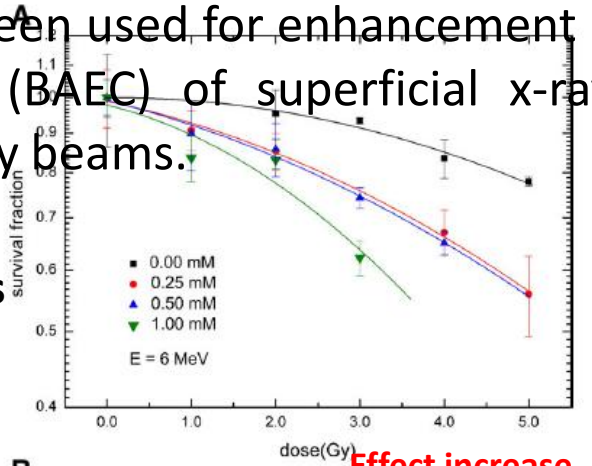

Indicates energy dependence

Dose enhancement factors at 90% cell survival

Type of irradiation	Energy	AuNPs concentration 0.25 mM	0.5 mM	1 mM
X-ray	80 kVp	4.0	20.0	24.6
	50 kvp	–	1.4	2.2
Electron	6 MeV	2.7	2.9	4.0
	12 MeV	–	3.7	4.1

Uptake and toxicity of GNPs

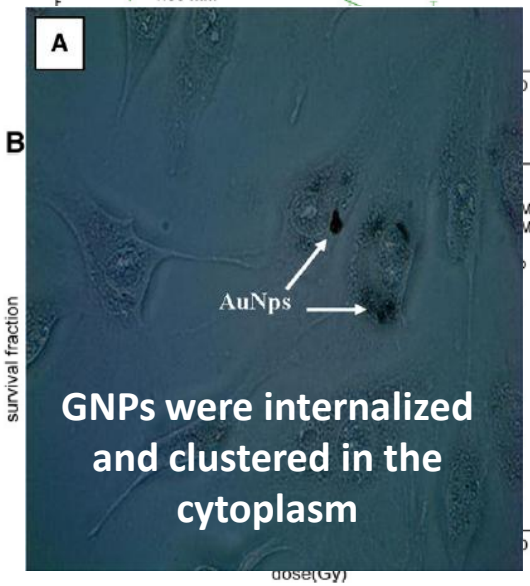

GNPs were internalized and clustered in the cytoplasm

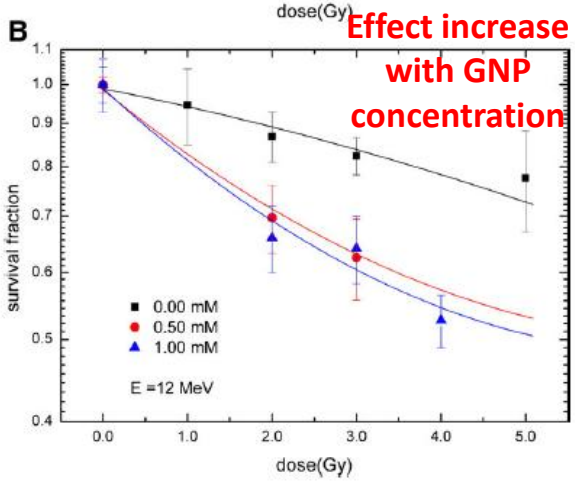

Effect increase with GNP concentration

Concentration dependence

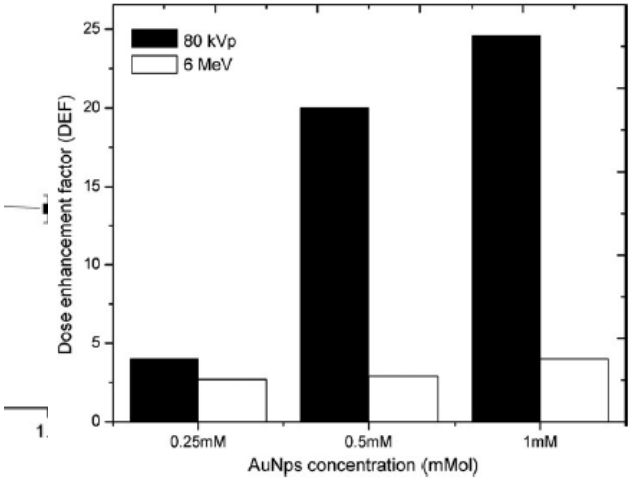

Rahman, W. N. et al. Nanomed- Nanotechnol. 2009,5: 136-142

In vitro studies

Jain et al. (2011)

The purpose of this [illegible] elevant MV x-ray energies. They incu[illegible]ncer MDA-MB-231 cells with GNPs and [illegible]ctron energies.

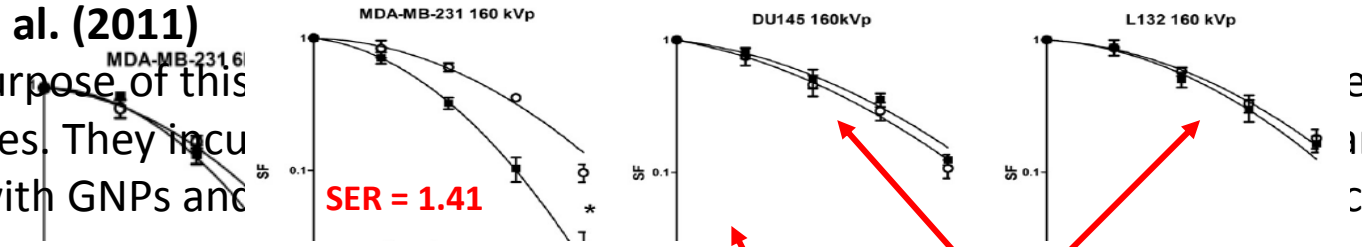

Table 1. Table of SERs, α, β, and SF_4 values for MDA-MB-231 cells with photons and electrons

				MDA-MB-231			DU145	L132
Radiation energy	Condition	α [Gy^{-1}]	β [Gy^{-2}]	SF_4	SER	p	SER	SER
160 kVp photons	Control	0.019 ± 0.025	0.052 ± 0.007	0.386	1.41	0.005	0.92	1.05
	GNP	0.091 ± 0.031	0.093 ± 0.011	[illegible]				
6 MV photons	Control	0.002 ± 0.022	0.079 ± 0.007	0.28	1.29	0.002	1.13	1.08
	GNP	0.104 ± 0.040	0.098 ± 0.011	0.12				
15 MV photons	Control	0.083 ± 0.027	0.059 ± 0.008	0.27	1.16	0.19		
	GNP	0.061 ± 0.050	0.121 ± 0.018	0.16				
6 MeV electrons	Control	0.05 ± 0.002	0.055 ± 0.008	0.029	1.04	0.62	1.12	0.97
	GNP	−0.088 ± 0.034	0.128 ± 0.013	0.18				
16 MeV electrons	Control	−0.038 ± 0.027	0.079 ± 0.008	0.3[illegible]		1.35	0.91	
	GNP	0.180 ± 0.036	0.015 ± 0.012	0.18				

Abbreviations: GNP = gold nanoparticle; SER = sensitizer enhancement ratio.

Not sensitization

In view of the sensitization observed with MV photons, they studied the effect of MV electrons to eliminate the effect of primary photon interactions with GNPs.

As in the photon irradiation experiments, sensitization was not observed in DU145 or L132 cells.

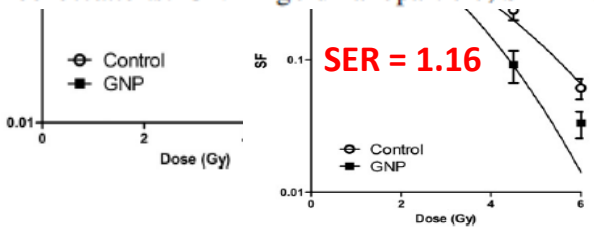

curves for [illegible] ıM GNP for 24 h.

with GNP at increasing photon energies: 160 kVp, 6MV and 15 MV..

Jain, S. et al. Int. J. Radiation Oncology Biol. Phys. 2011, 79: 531-539

In vitro studies

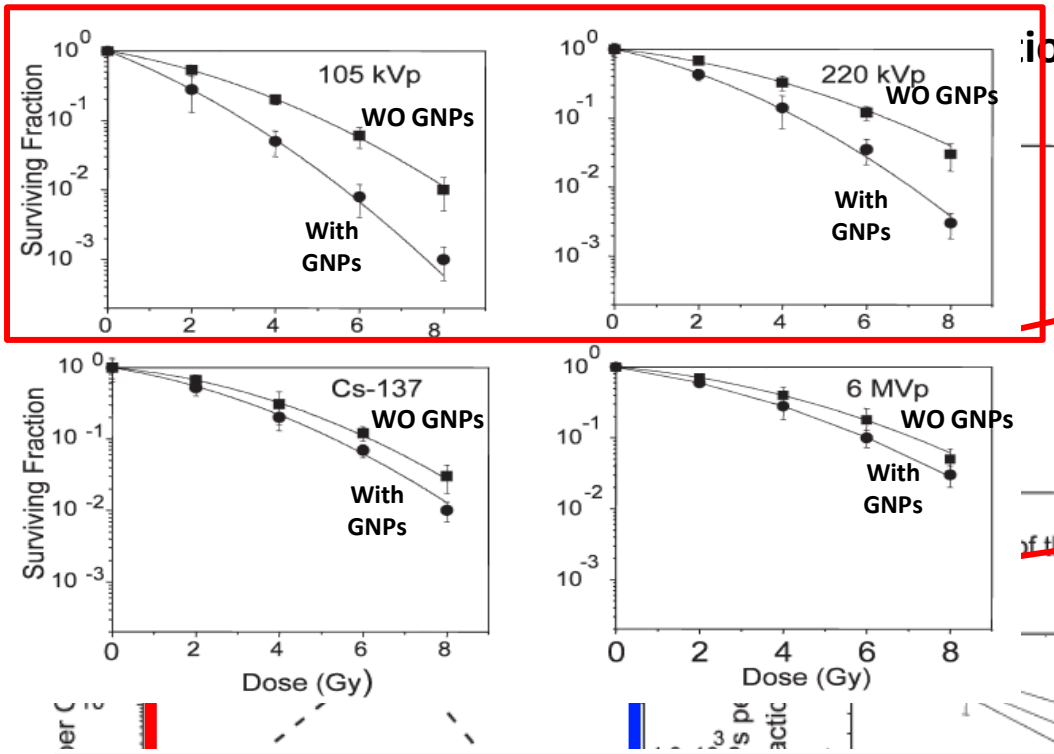

Greater radiation sensitization was seen for cells irradiated with the lower energy radiation beams

tion properties of
o various radiation
highest REF

The changes in sensitivity with gold nanoparticles are characterized by changes in the linear parameter (α) with no significant change in quadratic factor (β). This suggest that the effect is consistent with an increase in dose.

Related with cellular uptake

Related with the number of GNPs per

	105 kVp	220 kVp	^{137}Cs	6 MVp
$\alpha_{control}$	0.237 ± 0.005	0.150 ± 0.004	0.119 ± 0.013	0.110 ± 0.008
$\beta_{control}$	0.041 ± 0.002	0.041 ± 0.001	0.040 ± 0.003	0.029 ± 0.002
α_{gold}	0.528 ± 0.007	0.352 ± 0.005	0.259 ± 0.011	0.191 ± 0.002
β_{gold}	0.054 ± 0.003	0.041 ± 0.002	0.030 ± 0.003	0.031 ± 0.001
$\chi^2_{control}$	8×10^{-6}	1×10^{-5}	8×10^{-5}	6×10^{-5}
χ^2_{gold}	2×10^{-6}	4×10^{-6}	3×10^{-5}	1×10^{-6}
REF	1.66 ± 0.05	1.43 ± 0.02	1.18 ± 0.03	1.17 ± 0.02

Note. REFs were calculated as the ratio of doses without GNPs/dose with GNPs at 10% survival.

Chithrani, B. D. et al. Radiat. Res. 2010,173: 719-728

In vivo studies

In vivo studies

There are only a few *in vivo* reports of dose enhancing using gold nanoparticles:

- **Hainfeld et al. (2004):**

GNP on Balb/C mice bearing EMT-6 tumors injected with 1.9 nm GNP and exposed to 250 kVp x-rays

✓

- First *in vivo* experiment
- Big reduction of tumor volume
- Long term survival

✗

- High GNP concentrations
- High radiation doses
- Short time between injection and irradiation

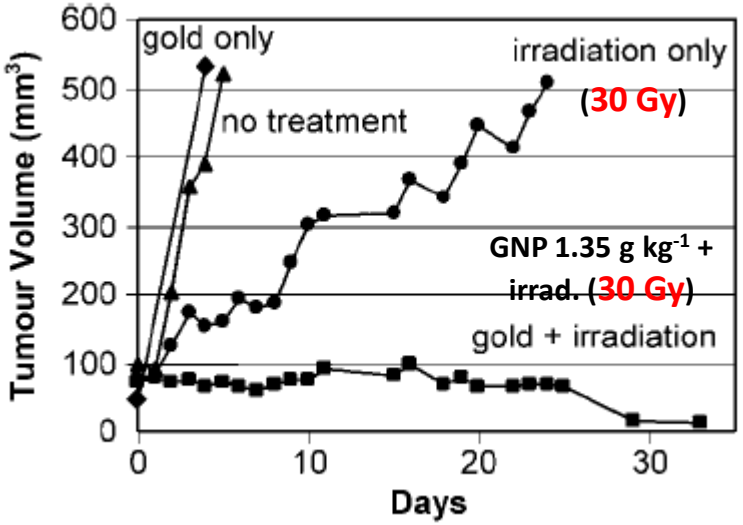

Table 1. Biodistribution of gold 5 min post i.v. injection of 1.35 g Au/kg.

	% injected dose/g	Tumour-to-tissue ratio	Tumour periphery-to-tissue ratio
Tumour	4.9 ± 0.6	1.0	1.8
Tumour periphery	8.9 ± 3.2	0.6	1.0
Muscle	1.4 ± 0.1	3.5	6.4
Liver	2.8 ± 0.1	1.8	3.2
Kidney	132.0 ± 2.7	0.4	0.1
Blood	18.6 ± 3.7	0.3	0.5

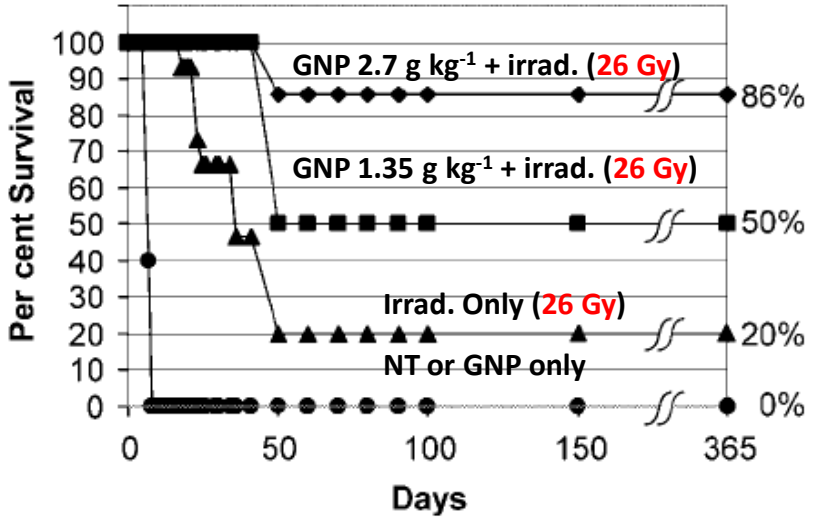

Hainfeld, J. F. et al. Phys. Med. Biol. 2004,49: N309-N315

In vivo studies

- **Chang et al. (2008):**

  GNP on C57BL/6 mice inoculated with mice melanoma B16F10 cells exposed to 13 nm GNP and 25 Gy of 6 MeV electron beams after 24 h incubation with GNP.

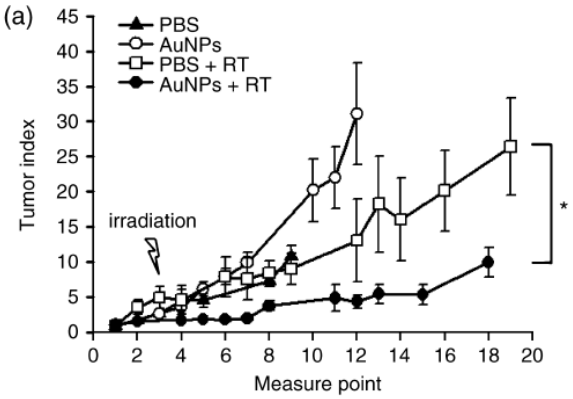

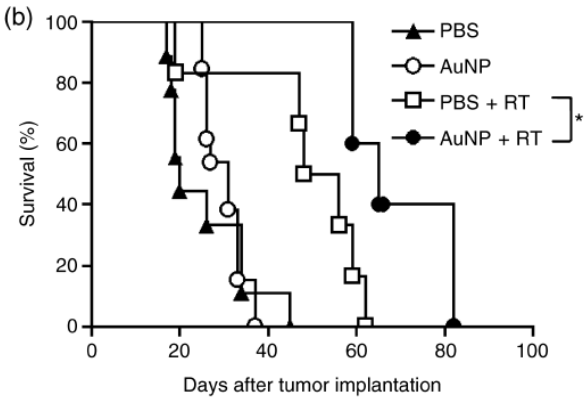

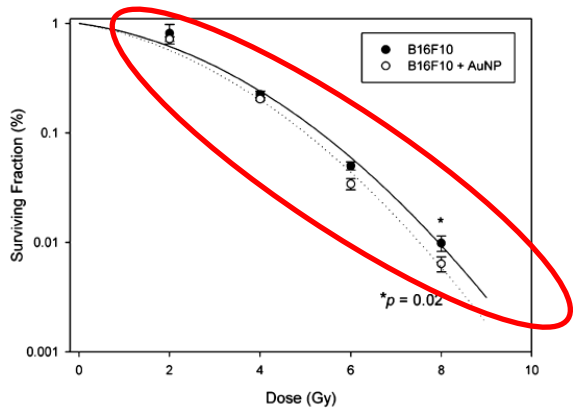

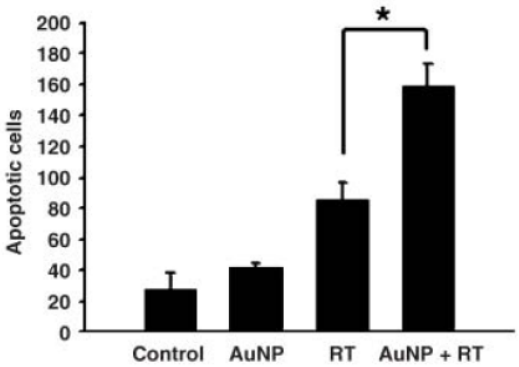

***In vitro* clonogenic assay**

- Tumor growth retarded
- Lower concentration of GNP than Hainfeld (2004)
- Longer time between injection and irradiation
- Significant increase in apoptosis
- Electron energies with clinical relevance.

- Little effect in *in vitro* clonogenic assay
- Shorter survival time

Chang, M-Y. et al. Cancer Sci. 2008,99: 1479-1484

In vivo studies

- **Alric et al. (2008):**

  They sinthesized GNP and functionalized it with Gd chelates to use it in x-ray imaging and radiotherapy.

  They injected rats bearing 9L gliosarcoma tumors with 2.4 nm DTDTPA-GNP and irradiated with 83 keV synchrotron x-rays

Series	n	MST days	MeST days
Control group	6	17.66 ±0.33	17.5
Au@DTDTPA-Gd_{50} + irradiation	8	33.25 ± 11.75	27.5

- DTDTPA-GNP crossed the brain blood barrier.
- Moderate contrast enhancement (15%)
- The irradiated rats exhibit larger survival times than non-treated rats.
- Weak toxicity.
- Pioneer work that combine x-ray imaging and x-ray therapy

- The skin entrance dose delivered was ~460 Gy
- Short time between injection and irradiation (20 min)

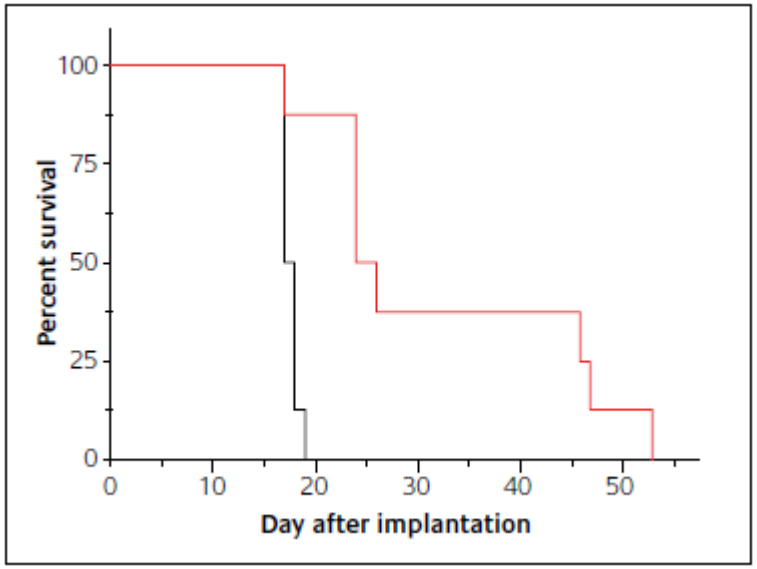

Alric, C. et al. Gold Bull. 2008,41: 90-97

In vivo studies

- **Hainfeld et al. (2010):**
  1.9 nm GNP in mice with radioresitant murine squamous cell carcinomas SCCVII irradiated with 68 keV synchrotron photons at different doses.

- Long-term tumor control using 68 keV at 42 Gy and 50.6 Gy
- Introduced hyperthermia (44°C for 20 min) to enhance radiation therapy

- No analysis of GNP tumor uptake or distribution
- High radiation doses

	Median (days)	Fraction surviving	p value[a]	p value[b]
A. 30 Gy, 68 keV				
−Gold	45	1/7 (14%)		
+Gold	44	1/7 (14%)		
30 Gy, 68 keV(−Gold) versus 42 Gy, 68 keV(−Gold)			$p > 0.1$	
30 Gy, 68 keV(+Gold) versus 42 Gy, 68 keV(+Gold)			$p < 0.02$	
B. 42 Gy, 68 keV				
−Gold	53	3/12 (25%)		
+Gold	76	8/12 (67%)		
42 Gy, 68 keV(−Gold) versus 42 Gy, 68 keV(+Gold)				$p < 0.04$
C. 44 Gy, 157 keV				
−Gold	29	0/7 (0%)		
+Gold	31	2/7 (29%)		
44 Gy, 157 keV (−Gold) versus 44 Gy, 157 keV(+Gold)			$p < 0.05$	
D. 50.6 Gy, 157 keV				
−Gold	31	0/8 (0%)		
+Gold	49	3/8 (38%)		
50.6 Gy, 157 keV(−gold) versus 50.6 Gy, 157 keV(+gold)			$p < 0.05$	

A. Heat only	Median (days) 7			Surviving fraction 0/7 (0%)		
	Median (days)			Surviving fraction		
	Radiation alone	Radiation + heat	Radiation + heat + gold	Radiation alone	Radiation + heat	Radiation + heat + gold
B. 1 × 15 Gy	11	25	32	0/7	1/10 (10%)	1/9 (11%)
C. 1 × 23 Gy	7.5	38.5	66	0/7	3/7 (43%)	3/6 (50%)
D. 2 × 15 Gy	ND	18	31.5	ND	8/20 (40%)	6/8 (75%)
E. 1 × 30 Gy	45		52	1/7 (14%)	7/7 (100%)	11/14 (79%)

Hainfeld, J. F. et al. Phys. Med. Biol. 2010,55: 3045-3059

In vivo studies

In vivo studies of GNP radiosensitization with ionizing radiation

Author	Year	GNP	GNP dose	Time to RT	Cell line	Radiation	Dose	Outcome measure	Group	Outcome	p-value
Hainfeld et al.	2004	1.9 nm	0 g Kg^{-1} 1.35 g kg^{-1} 1.35 g kg^{-1} 2.7 g kg^{-1}	2 min	EMT-6	256 kVp	26-30 Gy	Overall survival 1 year	GNP only RT only GNP+RT GNP+RT	0% 20% 50% 86%	0.01
Chang et al.	2008	13 nm	0 g kg^{-1} 1 g kg^{-1} 0 g kg^{-1} 1 g kg^{-1}	24 h	B16F10	6 MeV	25 Gy	Median survival	PBS GNP PBS+RT GNP+RT	45 days 40 days 60 days 80 days	<0.05
Alric et al.	2008	2.4 nm Au@DTDTPA-Gd_{50}	Au 50.7 mM	20 min	9L gliosarcoma	83 keV	~460 Gy	Mean survival time (MeST) Median survival time (MST)	Control Au@DTDTPA-Gd_{50} + irradiation	17.5 days MeST 17.66 days MST 27.5 days MeST 33.25 days MST	
Hainfeld et al.	2010	1.9 nm	0 g kg^{-1} 1.9 g kg^{-1}	~1 min	SCCVII	68 keV 157 keV	30 Gy 42 Gy 44 Gy 50.6 Gy	Doubling time	RT RT+GNP RT RT+GNP RT RT+GNP RT RT+GNP	45 days 44 days 53 days 76 days 29 days 31 days 31 days 49 days	<0.05 <0.05

In vivo studies

In vivo studies of GNP radiosensitization with ionizing radiation

Hainfeld studies showed the effective dose enhancement observed at the tumor sites.

The 68 keV and 157 keV photon beams showed improved tumor eliminating efficacy.

The 7 mg/kg gold concentration reported by Hainfeld, DEF values of over 1.60 were observed when using a 100 keV photon beam.

The effective dose enhancement dropped to 1.18 using a 250 keV photon beam and 1.05 when photon energy was increased to 500 keV.

The DEF values monotonically decreased as photon energy was increased and a minimum DEF of 1.003 was obtained using a 2.00 MeV photon beam.

Perspectives

The main perspective for the use of nanostructures for biomedical applications is to design a non-toxic multifunctional structure capable of be used for diagnostic, imaging and therapy.

There are great advances in some techniques like photothermal ablation, photodynamic therapy and the use of magnetic particles that had demostrated to minimize the damage caused to healthy tissue.

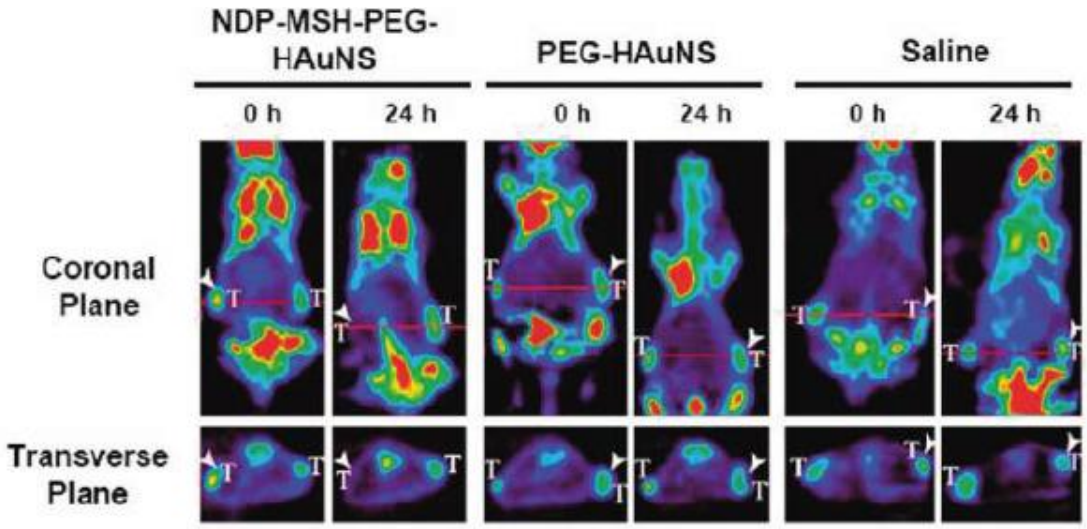

Lu, W. et al. Clin. Cancer. Res. 2009, 15:876-886

Perspectives

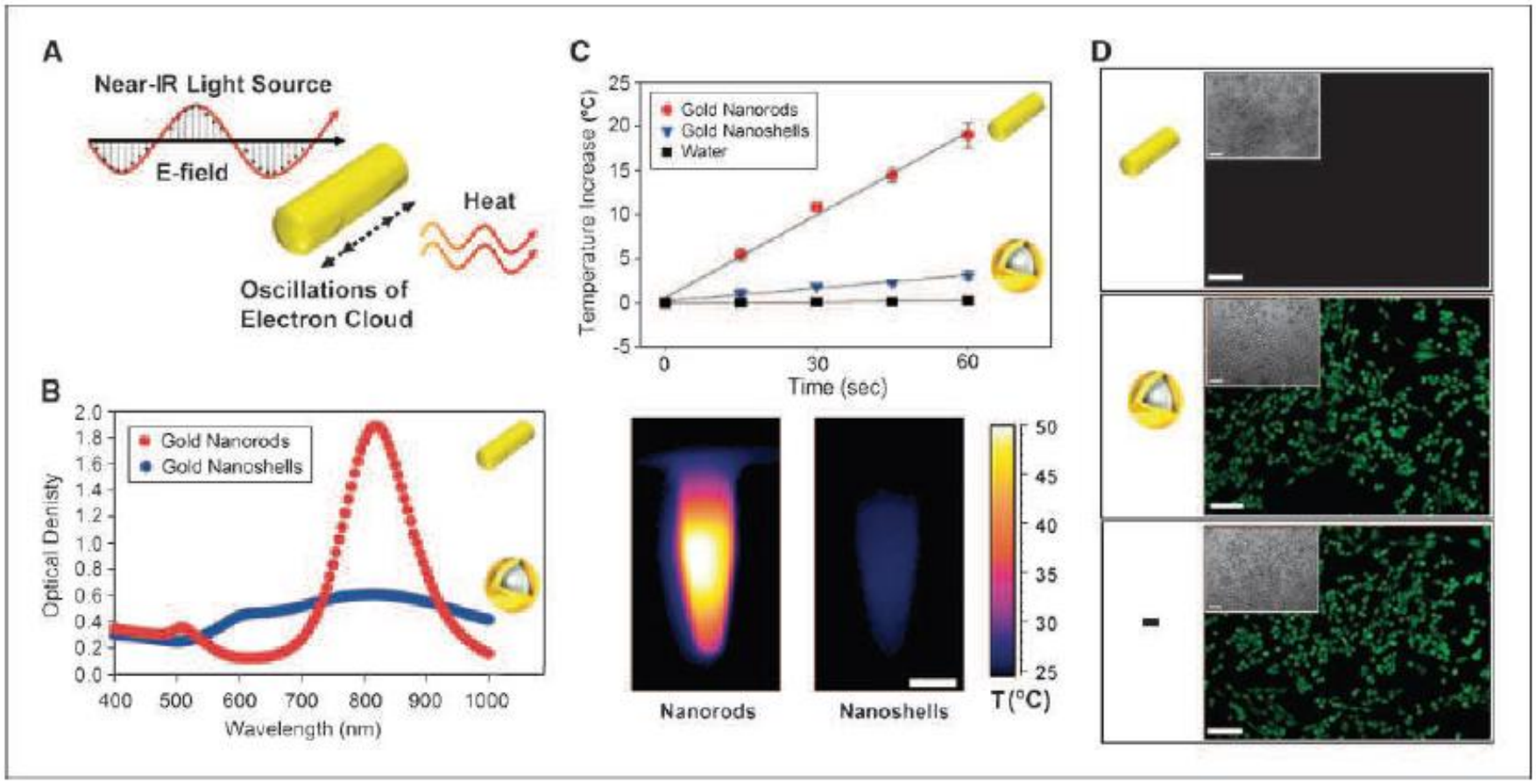

Figure 2. Spectral and photothermal properties of highly absorbing gold NRs compared with gold nanoshells. *A*, schematic of photothermal heating of gold NRs. The dimensions of gold NRs are tuned to have a near-IR plasmon resonance, at which point nanoparticle electrons resonantly oscillate and dissipate energy as heat. *B*, spectra for PEG-gold NRs (*red*) and PEG-gold nanoshells (*blue*), a benchmark for tunable plasmonic nanomaterials, at equal gold concentrations. *C*, *top*, rate of temperature increase for triplicate PEG-NR and PEG-gold nanoshell solutions (7 μg Au/mL, 810 nm laser, 2 W/cm^2, $n = 3$ each). *Bottom*, IR thermographic image of PEG-NRs versus PEG-gold nanoshells after 2 min of irradiation. *Scale bar*, 5 mm. *D*, *in vitro* photothermal toxicity of PEG-NRs over human cancer cells in culture (MDA-MB-435). Tumor cells were incubated with PEG-NRs (14 μg/mL; *top*), PEG-nanoshells (14 μg/mL; *middle*), or media alone (*bottom*) and treated with laser irradiation (2 W/cm^2, 810 nm, 5 min). Calcein AM staining indicates destruction of cells with PEG-NRs, whereas cells irradiated in the presence of nanoshells or media remained viable. Phase region of calcein staining inset. *Scale bar*, 10 μm.

Perspectives

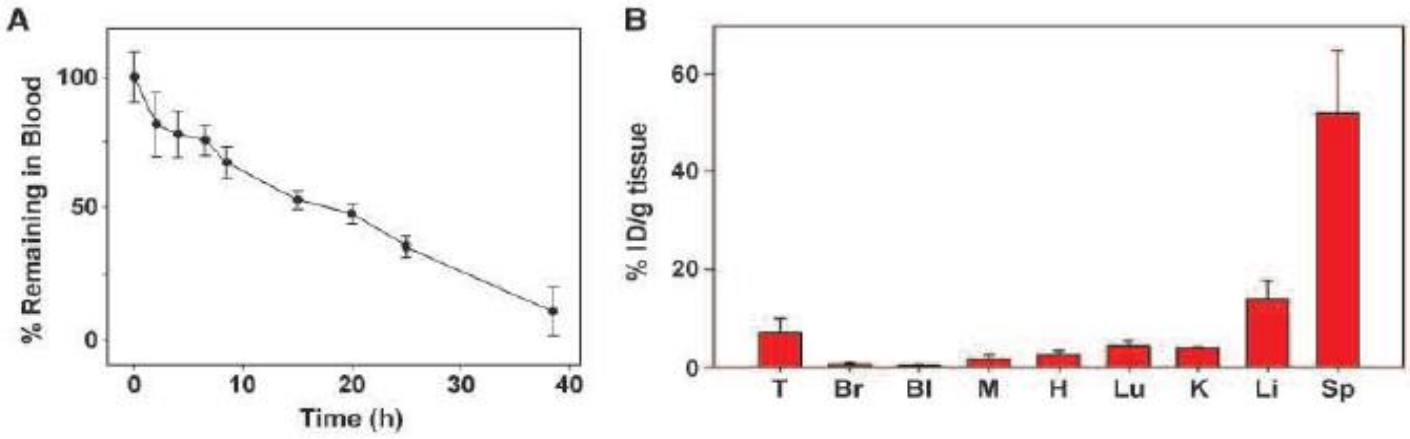

Figure 4. Long circulation time, passive tumor targeting, and photothermal heating of passively targeted gold NR antennas in tumors. *A*, PEG-NRs were i.v. given (20 mg/kg) to three mice bearing MDA-MB-435 tumors, and blood was withdrawn over time to monitor clearance from circulation. *B*, PEG-NR biodistribution and targeting to MDA-MB-435 tumors 72 h after i.v. administration, quantified via ICP-MS (three mice). *T*, tumor; *Br*, brain; *Bl*, bladder; *M*, muscle; *H*, heart; *Lu*, lung; *K*, kidney; *Li*, liver; *SP*, spleen. Data are tabulated in Supplementary Table S1. *C*, PEG-NRs or saline were i.v. given (20 mg/kg) to mice bearing MDA-MB-435 tumors on opposing flanks. After NRs had cleared from circulation (72 h after injection), the right flank was irradiated using an 810-nm diode laser (2 W/cm^2; beam size indicated by dotted circle). *D*, thermographic surveillance of photothermal heating in PEG-NR–injected (*top*) and saline-injected (*bottom*) mice.

Perspectives

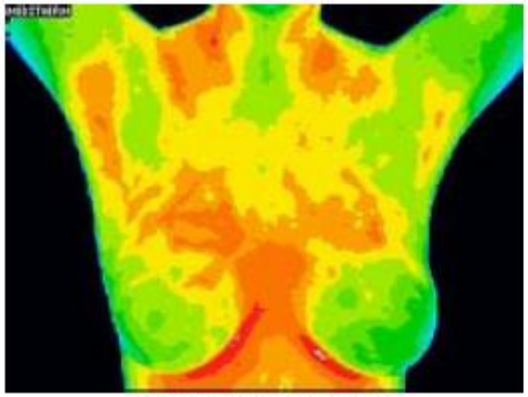

BARTAT021911A2BA

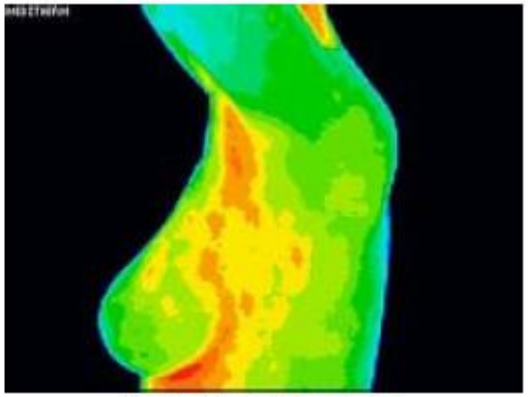

BARTAT021911A2BLL

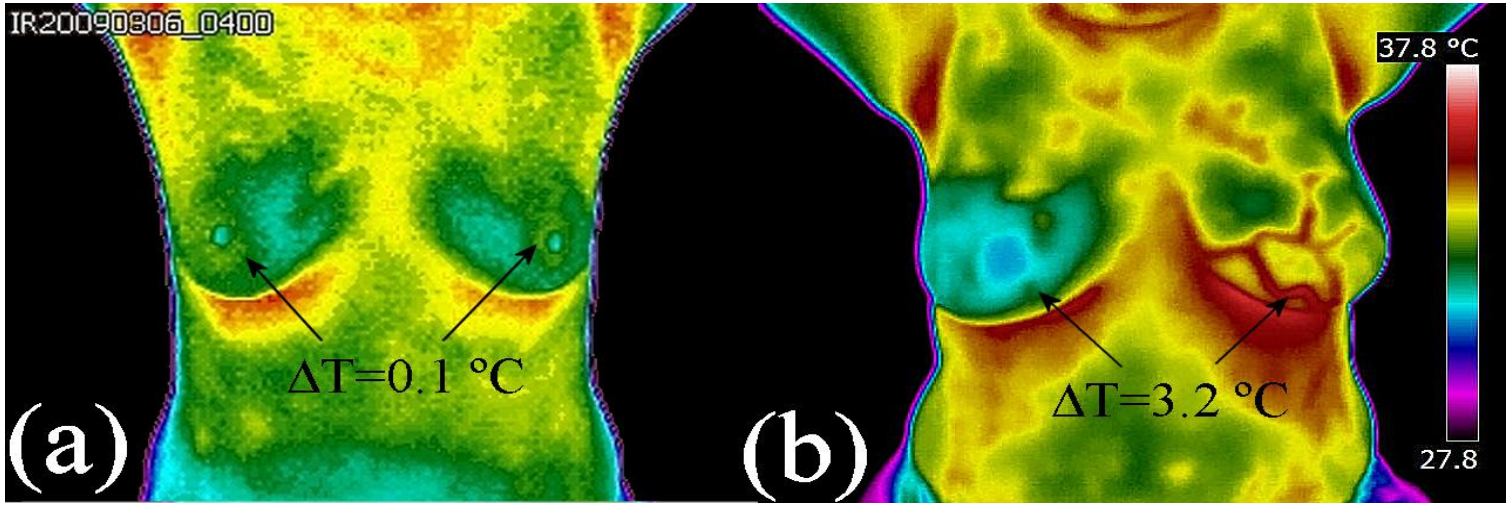

Conclusions

AuNPs are effective dose enhancers for superficial radiotherapy using kilovoltage x-ray beam and megavoltage electron beam.

The AuNPs enhanced the cells killing up to 15 times for 1 mMol/L of AuNPs irradiated with 80 kVp x-ray beams. Maximum dose enhancement factor (DEF) of 3 times was measured for 6 MeV electron beams in the presence of 1mMol/L AuNPs.

Minimal dose enhancement was observed for megavoltage photon beams which measured DEF are around 1 time (100% enhancement). Radiobiological analysis of the dose enhancement by AuNPs using linear quadratic model found systematic changes of alpha (α) value which increases with inclusion of AuNPs while there are very small changes for beta (β) value.

Results of the studies on the AuNPs cytotoxicity for different concentrations and sizes were found to be minimal. Viability tests and cell morphology studies show no significant effects of AuNPs to the cells.

Finally, AuNPs can potentially be applied as a novel radiobiological dose enhancer for radiation therapy, synchrotron based microbeam and stereotactic radiotherapy.

Thank you for your kind attention